Functional diversification of gram-negative intermembrane phospholipid transporters by intrinsic substrate preference

Ashutosh K. Rai[a], Katsuhiro Sawasato[b], Haley C. Bennett[a], Anastasiia Kozlova[b], Genevieve C. Sparagna[c], Mikhail Bogdanov[b], and Angela M. Mitchell[a,#]

[a] Department of Biology, Texas A&M University, College Station, Texas, USA

[b] Department of Biochemistry and Molecular Biology, McGovern Medical School at The University of Texas Health Science Center at Houston, Houston, Texas, USA

[c] Department of Medicine, Division of Cardiology, University of Colorado Anschutz Medical Campus, Aurora, Colorado, USA

Running title: Phospholipid transporter substrate preference

Address correspondence to Angela M. Mitchell, amitchell@bio.tamu.edu

Keywords: phospholipid trafficking, gram-negative envelope, outer membrane, lipid metabolism, cold sensitivity

Abstract

The outer membrane of Gram-negative bacteria is a barrier to chemical and physical stress. Phospholipid transport between the inner and outer membranes has been an area of intense investigation and, in *E. coli* K-12, it has recently been shown to be mediated by YhdP, TamB, and YdbH, which are suggested to provide hydrophobic channels for phospholipid diffusion, with YhdP and TamB playing the major roles. However, YhdP and TamB have different phenotypes suggesting distinct functions. We investigated these functions using synthetic cold sensitivity (at 30 °C) of a strain with deletion of *yhdP*, but not *tamB* or *ydbH*, and *fadR*, a transcriptional regulator controlling fatty acid degradation and unsaturated fatty acid production. Deletion of *tamB*, redirecting phospholipid transport to YdbH, suppresses the Δ*yhdP* Δ*fadR* cold sensitivity suggesting this phenotype is directly related to phospholipid transport. The Δ*yhdP* Δ*fadR* strain shows a greater increase in cardiolipin upon transfer to the non-permissive temperature and genetically lowering cardiolipin levels can suppress cold sensitivity. These data also reveal a qualitative difference between cardiolipin synthases in *E. coli*, as deletion of *clsA and clsC* suppresses cold sensitivity but deletion of *clsB* does not despite lower cardiolipin levels. In addition to increased cardiolipin, increased fatty acid saturation is necessary for cold sensitivity and lowering this level genetically or through supplementation of oleic acid suppresses the cold sensitivity of the Δ*yhdP* Δ*fadR* strain. A parsimonious explanation for our data is that YhdP and TamB have differential substrate transport preferences, most likely with YhdP preferentially transporting more saturated phospholipids and TamB preferentially transporting more unsaturated phospholipids. We envision cardiolipin contributing to this transport preference by sterically clogging TamB-mediated transport of saturated phospholipids. Thus, our data provide a potential mechanism for independent control of the phospholipid composition of the inner and outer membranes in response to changing conditions.

Author Summary

Gram-negative bacteria possess an impermeable outer membrane, which protects against environmental stress and antibiotics. Outer membrane phospholipid transport remained mysterious until recently when YhdP, TamB, and YdbH were implicated in phospholipid transport between the inner and outer membranes of *E. coli*. Similar roles for YhdP and/or TamB have been suggested in both closely and distantly related gram-negative bacteria. Here, given the transporters' apparent partial redundancy, we investigated functional differentiation between YhdP and TamB. Our data demonstrate that YhdP and TamB have differential involvement with fatty acid and phospholipid metabolism. In fact, transport of higher than normal levels of cardiolipin and saturated phospholipids by TamB at a non-permissive temperature is lethal. From these data, we suggest a model where the functions of YhdP and TamB are distinguished by their preference for phospholipid transport with YhdP preferentially transporting more saturated phospholipids and TamB transporting more unsaturated phospholipids. Cardiolipin headgroup specificity may contribute transport inhibition due to its bulky nature inhibiting the passage of other phospholipids. Diversification of function between YhdP and TamB provides a mechanism for regulation of phospholipid composition, and possibly the mechanical strength and permeability of the outer membrane, and so the cell's intrinsic antibiotic resistance, in changing environmental conditions.

Introduction

The gram-negative bacterial cell envelope has an outer membrane (OM) that sits outside the aqueous periplasm and peptidoglycan cell wall. The OM provides a barrier against various environmental stresses including toxic molecules such as antibiotics and osmotic pressure (1-6). Unlike the inner membrane (IM), a phospholipid bilayer, the OM is largely composed of phospholipids (mainly phosphatidylethanolamine (PE) (7)) in its inner leaflet and LPS (lipopolysaccharide) in its outer leaflet (2, 8). However, both membranes are asymmetric as the IM has different phospholipid compositions in its inner versus outer leaflets (9). Outer membrane proteins (OMPs) form a network across the cell surface interspersed with phase separated LPS patches (10). Lipoproteins are generally anchored in the inner (i.e., periplasmic) leaflet of the OM (11).

OM components are synthesized in the cytoplasm or IM and transported to the OM. OMP (12), lipoprotein (11), and LPS (13) transport pathways are well defined. However, until recently, intermembrane phospholipid transport (between the IM and OM), especially anterograde transport from the IM to the OM, has remained very poorly understood. Phospholipids are synthesized at the IM's inner leaflet (14) and rapid, bidirectional intermembrane phospholipid transport occurs (15), even without ATP (16). Phospholipid transport has a relaxed specificity, allowing transport of non-native lipids (17, 18); however, intermembrane phospholipid composition differences are maintained (7, 19-22). For instance, the OM is enriched for PE and its saturated species compared to the IM outer leaflet (7, 9, 20-22); however, PG and CL can be evenly distributed between the IM and OM when the cellular level of PE is greatly reduced (17), suggesting a maintenance of membrane charge balance. This headgroup redistribution was accompanied by a concomitant fatty acid redistribution evidenced by an accumulation of palmitic acid (C16:0) and cyclopropane derivatives of palmitoleic acid (C16:1) and *cis*-vaccenic acid (C18:1). In contrast, the 1,2-diglyceride that accumulates in mutants lacking DgkA (diglyceride kinase) predominantly associates with the IM (23), suggesting existence of a mechanism of discrimination of lipid transfer to the OM that does not recognize diglyceride molecules and contributes to the diversification of distribution of polar and acyl groups between the IM and OM. This establishment and maintenance of defined lipid topography between the IM and the OM must involve the coordinated biosynthesis and balanced bidirectional trafficking of specific phospholipids across the IM and from the IM to the OM (24).

It has been demonstrated that anterograde phospholipid transport is mediated by a high-flux, diffusive system in *Escherichia coli* (25). A retrograde trafficking pathway, the Mla system, removes mislocalized phospholipids from the OM outer leaflet and returns them to the IM (26). A gain-of-function allele, *mlaA** (27, 28), opens a channel allowing phospholipids to mislocalize to the cell surface by flowing from the OM's inner to outer leaflet (27, 29), resulting in a PldA (OM phospholipase A)-mediated attempt to reestablish OM asymmetry by increasing LPS production, OM vesiculation, and increased flow of

113 phospholipids to the OM (27, 28). When nutrients are depleted, inhibiting phospholipid
114 production, cells lyse due to loss of IM integrity (16, 18). Single cell imaging of *mlaA** cells
115 confirmed an aberrant lipid flow from the IM to the OM at a fast rate. Loss of YhdP, an
116 inner membrane protein, could significantly slow phospholipid flow to the OM resulting
117 in loss of OM integrity before IM rupture (25), suggesting YhdP might play a role in
118 intermembrane phospholipid transport.

119 Recently, YhdP and two homologs, TamB and YdbH, were demonstrated to be
120 intermembrane phospholipid transporters (30, 31). Ruiz, *et al*. investigated AsmA family
121 proteins and found Δ*yhdP* Δ*tamB* mutants showed synthetic OM permeability and
122 stationary phase lysis (30). Moreover, when combined, Δ*yhdP*, Δ*tamB*, and Δ*ydbH* are
123 synthetically lethal. Genetic interactions of these mutants with *mlaA* and *pldA* show their
124 involvement in OM phospholipid homeostasis. Predicted structures of YhdP, TamB, and
125 YdbH (32, 33), as well as a partial crystal structure of TamB (34), have a β-taco fold domain
126 with a hydrophobic pocket, resembling eukaryotic lipid transporters (35-38). These
127 structural findings are another clue that suggests YhdP, TamB, and YdbH are involved in
128 phospholipid transport. Douglass, *et al.* confirmed the synthetic lethality of Δ*yhdP*,
129 Δ*tamB*, and Δ*ydbH* and demonstrated a Δ*tamB* Δ*ydbH* mutant with reduced *yhdP*
130 expression had decreased amounts of OM phospholipids, directly demonstrating their
131 involvement in intermembrane phospholipid transport or its regulation (31). Structural
132 studies have shown that YhdP is long enough to span the periplasmic space and molecular
133 dynamics indicate that the C-terminus of YhdP can insert into the OM to allow
134 phospholipid transfer between the membranes (39). This study also directly
135 demonstrates that a phosphate containing substrate, putatively assigned to be
136 phospholipids, can be crosslinked to the hydrophobic groove of YhdP (39). The role of
137 YhdP, TamB, and YdbH in phospholipid transport may be widely conserved as recent
138 evidence implicates TamB in anterograde phospholipid transport in *Veillonella parvula*, a
139 diderm Fermicute (40) and YhdP, TamB, YdbH, and PA4735 in intermembrane
140 phospholipid transport in *Pseudomonas aeruginosa* (41).

141 Nevertheless, why there are three separate intermembrane phospholipid transport
142 proteins and the functional interactions between these proteins remains unanswered,
143 although it is clear the proteins are not fully redundant or functionally equivalent. The
144 conditional expression of *yhdP* alone, without the presence of *ydbH* and *tamB*, fully
145 complements neither growth phenotypes nor a normal level of OM phospholipids,
146 suggesting transport function is still impaired in this strain (31). In addition, YdbH seems
147 to play a more minor role than YhdP and TamB (30, 31) and the screen identifying Δ*yhdP*
148 as slowing *mlaA**-dependent lysis did not identify Δ*tamB* or Δ*ydbH* (25). Moreover, we
149 previously identified a role for YhdP in stationary phase SDS (sodium dodecyl sulfate)
150 resistance and modulating cyclic enterobacterial common antigen activity (42, 43) not
151 shared by TamB and YdbH (**Fig. S1**) (30, 31, 42, 43). Similarly, TamB, in conjunction with

152 TamA, has been suggested to play a role in OM insertion of some "complicated" β-barrel
153 OMPs such as autotransporters and usher proteins (34, 44-46).

154 Here, we investigated the differentiation of YhdP and TamB function and identified
155 synthetic cold sensitivity in a strain with Δ*yhdP* and Δ*fadR*, a transcriptional regulator of
156 fatty acid biosynthesis and degradation, acting as a transcriptional switch between these
157 pathways in response to acyl-CoA (47). FadR is necessary for normal levels of unsaturated
158 fatty acids to be synthesized (48). The cold sensitivity was unique to the Δ*yhdP* Δ*fadR*
159 strain and was suppressed by loss of TamB, demonstrating that the sensitivity is related
160 to phospholipid transport. We found that the Δ*yhdP* Δ*fadR* mutant had a greater increase
161 in levels of a specific phospholipid, cardiolipin (CL) during growth at the non-permissive
162 temperature, and decreasing CL suppressed cold sensitivity. Furthermore, increasing
163 unsaturated fatty acid levels suppressed cold sensitivity. Overall, our data are consistent
164 with a model where TamB and YhdP transport functions are differentiated based on
165 phospholipid fatty acid saturation state, with TamB transporting more unsaturated
166 phospholipids and YhdP transporting more saturated phospholipids. Phospholipid species
167 or head group can also contribute to transport specificity, since higher levels of dianionic
168 CL are necessary for the cold sensitivity phenotype, potentially due to functional
169 inhibition of TamB by clogging of its hydrophobic groove.

170

171

172 **Results**

173 **Loss of FadR and YhdP results in cold sensitivity suppressed by loss of TamB.** To
174 investigate YhdP-TamB function differentiation, we created a Δ*yhdP* Δ*fadR* strain, as FadR
175 is a major regulator of lipid homeostasis (47). A deletion strain of *fadR* alone is expected
176 to have decreased fatty acid synthesis, increased fatty acid degradation, and increased
177 fatty acid saturation (47, 48). Surprisingly, Δ*yhdP* Δ*fadR* cultures grown at 30 °C lagged for
178 more than 8 hours, followed by highly variable growth, suggesting suppressor outgrowth
179 (**Fig.1A**). The growth defect was decreased at 37 °C and completely absent at 42 °C. To
180 confirm this cold sensitivity, we estimated efficiency of plating (EOP) and confirmed the
181 severe cold intolerance of the Δ*yhdP* Δ*fadR* strain (5 logs at 30 °C and 3 logs at 37 °C) (**Fig.
182 1B**). Although, enterobacterial common antigen is necessary for Δ*yhdP*'s OM permeability
183 phenotypes (43), the Δ*yhdP* Δ*fadR* strain's cold sensitivity was unchanged when
184 enterobacterial common antigen was not present (Δ*wecA*) (49) (**Fig. 1C**).

185 We hypothesized the Δ*yhdP* Δ*fadR* strain's cold sensitivity was due to impairment of
186 phospholipid transport and expected Δ*tamB* and/or Δ*ydbH* to show similar synthetic
187 phenotypes with Δ*fadR*. However, Δ*fadR* Δ*tamB* and Δ*fadR* Δ*ydbH* strains had no growth
188 defects (**Fig 1D**). Although Δ*ydbH* in the Δ*yhdP* Δ*fadR* strain did not alter cold sensitivity
189 (**Fig. 1E**), Δ*tamB* in the Δ*yhdP* Δ*fadR* background completely suppressed the cold
190 sensitivity (**Fig. 1F**). Consistent with previous observations (30), the Δ*yhdP* Δ*fadR* Δ*tamB*
191 strain was mucoid due to Rcs (regulator of capsule synthesis) stress response activation

192 and colanic acid capsule production. Deleting *rcsB*, an Rcs response regulator, prevented
193 mucoidy but did not affect suppression (**Fig. 1F**). We observed only minimal growth
194 phenotypes in the Δ*yhdP* Δ*fadR* Δ*tamB* strain, similar to those of Δ*tamB* and less severe
195 than those of Δ*fadR* (**Fig. 1G**), making slow growth an unlikely suppression mechanism.
196 Together, these data demonstrate the Δ*yhdP* Δ*fadR* strain has impaired phospholipid
197 transport leading synthetic cold sensitivity, which can be relieved by deletion of Δ*tamB*,
198 shifting phospholipid transport to YdbH.

199 We next looked for envelope homeostasis alterations in the Δ*yhdP* Δ*fadR* strain. To
200 identify cell lysis and/or severe OM permeability defects at 30 °C, we assayed CPRG
201 (chlorophenol red-β-D-galactopyranoside) processing. CPRG must contact LacZ in the
202 cytoplasm or supernatant to release chlorophenol red (50). Compared to wild type or
203 single mutants, the Δ*yhdP* Δ*fadR* strain had increased CPRG processing (**Fig. S2A**),
204 demonstrating lysis or increased envelope permeability. When we assayed resistance to
205 molecules excluded by the OM (1, 42, 43, 51, 52) at 37 °C, a semi-permissive temperature,
206 the Δ*yhdP* Δ*fadR* strain showed sensitivity to vancomycin, a large scaffold antibiotic, and
207 SDS EDTA compared to single mutants (**Fig. S2B**). However, with bacitracin treatment or
208 EDTA treatment alone, the Δ*yhdP* Δ*fadR* strain phenocopied the Δ*fadR* single deletion
209 (**Fig. S2CD**). LPS levels were not altered in the Δ*yhdP*, Δ*fadR*, or the Δ*yhdP* Δ*fadR* strain
210 (**Fig. S2E**). OM asymmetry mutations (i.e., Δ*pldA*, Δ*mlaA*) (26-28, 53) did not have
211 suppressive or synthetic effects on cold sensitivity in the Δ*yhdP* Δ*fadR* strain (**Fig. S3AB**),
212 suggesting against a causal loss of OM asymmetry. Overall, the changes in OM
213 permeability did not seem sufficient to cause lethality at lower temperature, suggesting
214 the phospholipid transport disruption affects both IM and OM integrity.

215 **Increased cardiolipin is necessary for cold sensitivity.** We investigated phospholipid
216 composition of the wild-type, Δ*yhdP*, Δ*fadR*, and Δ*yhdP* Δ*fadR* strains grown at the
217 permissive temperature (42 °C) to log phase then downshifted to 30 °C. *E. coli*
218 phospholipid composition is generally 75% phosphatidylethanolamine (PE), 20%
219 phosphatidylglycerol (PG), and 5% cardiolipin (CL) with CL increasing in stationary phase
220 (14, 54). Of the three CL synthases, ClsA and ClsB synthesize CL from two PG molecules,
221 while ClsC synthesizes CL from one PG and one PE molecule, so CL and PG levels are
222 generally reciprocally regulated (55-58). For all strains, the levels of PE were similar (**Fig.
223 2A**, **Fig. S4A**). However, the Δ*yhdP* Δ*fadR* strain had increased CL and concomitant
224 decreased PG compared to the wild-type strain and compared to individual Δ*yhdP* and
225 Δ*fadR* mutants (**Fig. 2B**). PgsA synthesizes phosphatidylglycerol-phosphate and is the first
226 enzyme differentiating PG and PE biosynthesis. PgsA depletion would decrease both PG
227 and CL levels, reversing increased CL levels and exacerbating decreased PG levels in the
228 Δ*yhdP* Δ*fadR* strain. We tested the effect of PgsA depletion in a strain background (Δ*rcsF*
229 Δ*lpp*) where *pgsA* is non-essential (59-62). When *pgsA* expression was induced (arabinose
230 panel), the Δ*yhdP* Δ*fadR* PgsA-depletion strain had equal cold sensitivity to the Δ*yhdP*
231 Δ*fadR* strain (**Fig. 2C**). When *pgsA* expression was repressed (glucose panel), the Δ*yhdP*
232 Δ*fadR* cold sensitivity was partially suppressed, demonstrating that decreased PG does

233 not cause cold sensitivity and suggesting increased CL may be necessary for cold
234 sensitivity. Indeed, the cold sensitivity of the Δ*yhdP* Δ*fadR* strain was lost when CL was
235 fully depleted due to deletion of the genes for all cardiolipin syntheses (Δ*clsABC*) or of the
236 gene for the primary cardiolipin synthase (Δ*clsA*) responsible for CL synthesis in
237 exponential phase (**Fig. 2ADE**, **Fig. S4B**). Δ*clsB* caused a smaller decrease in CL levels, while
238 Δ*clsC* did not cause a decrease (**Fig. 2AB**, **Fig. 4B**). Surprisingly, however, Δ*clsC* completely
239 suppressed the cold sensitivity, while Δ*clsB* did not (**Fig. 2FG**). Thus, increased CL is
240 necessary for cold sensitivity but CL levels alone cannot explain the phenotype: another
241 factor, such as a specific molecular form (e.g., acyl chain length, saturation state,
242 symmetry of acyl chain arrangement) or localization (e.g., poles vs. midcell or inner vs.
243 outer leaflet) of CL, is required.

244 **Increased *fabA* expression suppresses cold sensitivity.** To identify other factors involved
245 in the cold sensitivity, we applied a forward genetic approach by isolating spontaneous
246 suppressor mutants capable of growing at 30 °C and identified a suppressor mutant
247 (Suppressor 1) that restored growth at 30 °C (**Fig. 3A**), decreased CPRG processing (**Fig.**
248 **S2A**), and had very similar CL to the Δ*yhdP* Δ*fadR* strain (**Fig. 3AB**, **Fig. S4A**). We identified
249 a point mutation in the *fabA* promoter region in Suppressor 1 (**Fig. 3B**) and confirmed this
250 mutation was sufficient for suppression (**Fig. 3C**). FabA is a dehydratase/isomerase that
251 introduces *cis* unsaturation into fatty acids (14, 63) and *fabA* is expressed from two
252 promoters controlled by FadR and FabR (64, 65). FadR activates *fabA* expression, while
253 FabR represses. Thus, *fadR* deletion would be expected to lower *fabA* expression. The
254 suppressor mutation was located in the *fabA* promoter FabR binding site (**Fig. 3B**) and we
255 hypothesized this mutation would increase *fabA* expression. *fabA* mRNA levels were more
256 than 4-fold lower in the Δ*yhdP* Δ*fadR* strain than the wild-type strain (**Fig. 3D**). While
257 lower than wild type, the suppressor mutant increased *fabA* mRNA 1.6-fold over the
258 Δ*yhdP* Δ*fadR* strain.

259 We constructed luciferase reporter plasmids with the wild-type *fabA* promoter region or
260 the *fabA* promoter region containing the suppressor mutation. The reporter with the
261 mutated promoter had higher activity in a wild-type, Δ*fadR,* and Δ*fabR* background (**Fig.**
262 **3E**). *fabA* transcription occurs from a promoter downstream of the FabR binding site (65-
263 67). However, when *fadR* is deleted, transcription shifts to the FabR-regulated promoter
264 within the FabR binding region (65-67). Our data indicate the Suppressor 1 mutation
265 regulates this promoter's constitutive activity rather than FabR binding. To confirm the
266 effect of changing the second promoter's activity, we tested the effect of Δ*fabR* on cold
267 sensitivity in the Δ*yhdP* Δ*fadR* strain and observed partial suppression (**Fig. S5**). The
268 smaller effect of Δ*fabR* compared to Suppressor 1 may result from other gene expression
269 changes or to the smaller relative effect of Δ*fabR* on *fabA* expression (**Fig. 3F**). Overall,
270 these data demonstrate increasing *fabA* expression, which is necessary for unsaturated

271 fatty acid biosynthesis, rescues cold sensitivity in the Δ*yhdP* Δ*fadR* strain without changing
272 CL levels.

273 **Increasing unsaturated fatty acids relieves cold sensitivity.** Given the effect of *fabA*
274 expression on the Δ*yhdP* Δ*fadR* cold sensitivity, we used liquid chromatography-
275 electrospray ionization mass spectrometry (LC/MS) to characterize the strains'
276 phospholipid saturation state (**Dataset S1**, **Fig. 4A-D**). Representitive spectra
277 demonstrating relative phospholipid composition are shown in **Fig. S6**. As expected,
278 Δ*fadR* caused increased fully saturated and monounsaturated PE and PG with a
279 concomitant decrease of diunsaturated PE (**Fig. 4AB**). Similarly, the Δ*fadR* strain
280 demonstrated increased monounsaturated CL with a concomitant decrease in
281 triunsaturated CL (**Fig. 4C**). Compared to the Δ*fadR* strain, the Δ*yhdP* Δ*fadR* strain had
282 slightly decreased saturation for all three phospholipids, while still displaying more
283 phospholipid saturation than wild type or Δ*yhdP* strains (**Fig. 4A-C**). Suppressor 1 trended
284 towards decreased saturation of all three phospholipids compared to the Δ*yhdP* Δ*fadR*
285 strain (**Fig. 4A-C**). We wondered whether the suppression difference between Δ*clsC* and
286 Δ*clsB* resulted from the CL saturation state. However, the Δ*yhdP* Δ*fadR* Δ*clsB* and Δ*yhdP*
287 Δ*fadR* Δ*clsC* strains had very similar CL profiles (**Fig. 4C**), suggesting another qualitative
288 difference affecting suppression, perhaps CL lateral or inter-leaflet distribution in the cell.
289 These strains also showed similar PE and PG saturation profiles to their Δ*yhdP* Δ*fadR*
290 parent (**Fig. 4AB**).

291 We hypothesized increasing unsaturated fatty acids suppresses Δ*yhdP* Δ*fadR* cold
292 sensitivity and performed EOPs for cold sensitivity on media containing an unsaturated
293 fatty acid (oleic acid, C18:1 *cis*-9). Exogenous phospholipids can be taken up by *E. coli*,
294 attached to acyl-CoA, and incorporated into phospholipids (68). Oleic acid addition
295 suppressed the Δ*yhdP* Δ*fadR* strain's cold sensitivity (**Fig. 4D**). Supplementing oleic acid
296 increases unsaturated phospholipids and provides an exogenous fatty acid source. To
297 differentiate between saturation state and fatty acid availability, we compared treatment
298 with oleic acid and saturated stearic acid (C18:0). Only oleic acid, and not stearic acid,
299 suppressed the Δ*yhdP* Δ*fadR* strain's cold sensitivity (**Fig. 4E**), confirming increasing
300 unsaturated fatty acids, not fatty acid availability suppresses.

301 **Suppression causes fatty acid metabolism and stress response alterations.** In wild-type
302 cells, *fabA* overexpression does not change phospholipid saturation levels, demonstrating
303 the FabB enzyme is rate limiting for unsaturated fatty acid biosynthesis (69). We were
304 intrigued that Suppressor 1 altered saturation without directly effecting *fabB* expression.
305 We also wondered whether CL levels in the Δ*yhdP* Δ*fadR* strain are transcriptionally
306 regulated. Thus, we investigated the transcriptional landscape of the wild type, the Δ*yhdP*
307 Δ*fadR*, and Suppressor 1 strains after a 30 minute downshift of growth to 30 °C to
308 determine: (i) whether the Δ*yhdP* Δ*fadR* strain had altered *cls* gene expression; (ii)
309 whether Suppressor 1 had other transcriptional changes; and (iii) why increased *fabA*
310 expression decreased saturation. All differentially expressed genes (>2-fold change,

311 p<0.05) are listed in **Dataset S2**. Principle component analysis of these genes showed the
312 closest relation between Δ*yhdP* Δ*fadR* strain and Suppressor 1, while the wild-type strain
313 was more distantly related (**Fig. 5A**, **S7A**). Nevertheless, Suppressor 1 was more closely
314 related to wild type than was the Δ*yhdP* Δ*fadR* strain. Most differentially regulated genes
315 between Δ*yhdP* Δ*fadR* and wild type and Suppressor 1 and wild type were upregulated
316 (**Fig. 5BC**, **S7BC**). Many of the most highly regulated genes are FadR-regulon members.
317 The majority of differentially regulated genes in Suppressor 1 compared to Δ*yhdP* Δ*fadR*
318 are downregulated (**Fig. 5D, S7D**). These genes are involved in many cellular pathways
319 and likely reflect the decreased cellular stress (**Table S2**). Indeed, many external stress
320 response genes are more enriched in Δ*yhdP* Δ*fadR* than in Suppressor 1 (**Fig. S8A**).

321 No significant expression changes occurred in the CL biosynthesis pathway (**Fig. 5E**) or
322 other phospholipid biosynthesis genes (**Fig. S8B**). The increased cardiolipin in Δ*yhdP*
323 Δ*fadR* and Suppressor 1 may be post-transcriptional or due to a change in a regulatory
324 pathway not yet altered after 30 minutes at 30 °C (**Fig. S8C**). Levels of mitochondrial CL
325 can be altered due to differences in substrate binding affinity of the CL synthase based on
326 saturation, with increased saturation decreasing CL synthesis (70), and it may be that a
327 similar pathway operates here, albeit in a different direction. We examined the
328 expression of genes in fatty acid synthesis and degradation, many of which are members
329 of the FadR regulon. In Δ*yhdP* Δ*fadR* compared to wild type, many fatty acid biosynthesis
330 genes significantly decreased while many fatty acid degradation genes significantly
331 increased (**Fig. 5F**), consistent with Δ*fadR* effects. While *fabA* expression is decreased,
332 *fabB* expression is not changed, explaining why increased *fabA* expression causes
333 decreased saturation in Suppressor 1. Overall, our data demonstrate the Δ*yhdP* Δ*fadR*
334 strain's cold sensitivity is due to impaired phospholipid trafficking, and increased
335 phospholipid saturation and cardiolipin are necessary for this functional impairment.
336
337
338 **Discussion**
339 The identification of YhdP, TamB, and YdbH as putative intermembrane phospholipid
340 transporters (30, 31) posed the tantalizing question: why is having three transporters
341 advantageous? Differential phenotypes between the transporters suggest that they
342 possess specialized functions (25, 30, 31, 34, 43-46). Here, we demonstrate each protein
343 plays a distinguishable role in phospholipid transport that can be differentiated based on
344 genetic interactions with lipid metabolism. Disruption of FadR and YhdP function causes
345 synthetic cold sensitivity not shared by TamB or YdbH, which can be suppressed by
346 removing TamB and switching transport to YdbH. This phenotype requires both increased
347 levels of CL and saturated fatty acids, and decreasing amounts of either suppresses. In
348 addition, our data demonstrate that CL synthesized by ClsB and ClsC is qualitatively
349 different—resulting in differential suppression phenotypes—likely due to differences in
350 CL localization, CL-mediated, leaflet-specific changes in lipid packing order (9, 24),
351 localized membrane fluidity (71), or TamB interaction.

352 Based on these data, we now suggest a model for the differentiation of function between
353 YhdP and TamB that leads to their independent phenotypes (**Fig. 6A-C**). In this model, the
354 functions of YhdP and TamB are diversified based on the acyl carbon saturation level
355 preference of the phospholipids they transport: YhdP transports mainly phospholipids
356 with more saturated fatty acids, while TamB transports phospholipids with more
357 unsaturated fatty acids (**Fig. 6A**). Our data and previous data (30, 31) agree YdbH plays a
358 relatively minor role. In the Δ*yhdP* Δ*fadR* strain, YhdP's absence forces more saturated
359 phospholipids to be transported by TamB. At 30 °C, TamB becomes "clogged" by
360 phospholipids having more saturated fatty acyl side chains, impeding transport (**Fig. 6B**).
361 This cold-specific effect may occur due to (i) temperature-dependent decreased
362 membrane fluidity and higher lipid packing order involving lower expression of FabF (**Fig.
363 5F**, **Dataset 3**), which is responsible for increased diunsaturated phospholipids at lower
364 temperature (14); (ii) higher relative levels of CL (72); (iii) higher amounts of per cell
365 phospholipids at lower temperatures (72) contributing to increased diffusive flow rate;
366 or, (iv) to thermodynamic properties altering TamB transport specificity and/or substrate
367 behavior contributing to efficiency of substrate loading or transport. Bulky and
368 intrinsically disordered CL molecules could contribute to the clogging sterically by
369 obstructing the lipid channel and precluding it from translocating other lipid substrates
370 (i.e., PE). YdbH's ability to successfully transport phospholipids in the Δ*yhdP* Δ*tamB* strain
371 only when TamB is absent may be because YhdP and TamB are primary transporters (e.g.,
372 preferred interaction partners for other pathway members), due to direct toxicity caused
373 by TamB clogging, or because *ydbH* is upregulated in the absence of the other
374 phospholipid transporters.

375 Several pieces of evidence demonstrate dysregulation of phospholipid transport not just
376 changes to OM phospholipid composition, and so permeability or physical strength, cause
377 the cold sensitivity phenotype of the Δ*yhdP* Δ*fadR* strain. First, the cold sensitivity is
378 unaffected by removing enterobacterial common antigen, which suppresses the
379 membrane permeability of a Δ*yhdP* strain (**Fig. 1C**, (43)), and the OM permeability
380 phenotypes of the Δ*yhdP* Δ*fadR* are not severe (**Fig. S2**). Second, the cold sensitivity is
381 suppressed by deletion of Δ*tamB* (**Fig. 1FG**). Δ*yhdP* Δ*tamB* strains have much greater OM
382 permeability (30) than the Δ*yhdP* or Δ*yhdP* Δ*fadR* strains. Third, CL has been shown to
383 have a normalizing, bidirectional, and leaflet-specific effect on lipid packing order (9, 73-
384 76) and membrane fluidity (77-80) opposite of or similar to that of cholesterol,
385 respectively, and so is unlikely to contribute to a phenotype dependent solely on OM
386 membrane fluidity. Thus, the cold sensitivity phenotype correlates with the impairment
387 of phospholipid trafficking and the likely imbalance of phospholipids between the IM and
388 OM and not with the permeability phenotypes of the OM.

389 Although both fatty acid saturation and high CL levels are required for the Δ*yhdP* Δ*fadR*
390 strain's cold sensitivity, two lines of evidence point to saturation rather than headgroup
391 as the main factor separating YhdP and TamB function. (i) YhdP loss slows phospholipid
392 transport from the IM to the OM in a *mlaA** mutant, which loses OM material due to

393 vesiculation and lysis when phospholipid biosynthesis is insufficient to replace lost
394 phospholipids (25, 27). CL only accounts for 5% of phospholipids in exponentially growing
395 cells making it unlikely that the loss of CL transport could slow net phospholipid transport
396 to the extent required to slow lysis. (ii) Δ*tamB* has a small growth defect at 30 °C (**Fig. 1G**)
397 not observed at higher temperature (30, 31), perhaps due to increased unsaturated
398 phospholipids (81-83) resulting in decreased net OM transport by YhdP or to lower OM
399 fluidity. Together, these observations provide strong evidence YhdP has a substrate
400 preference for phospholipids with more saturated fatty acids, while TamB prefers
401 phospholipids with more unsaturated fatty acids.

402 Our model suggests the IM and OM saturation state could be independently regulated
403 based on YhdP and TamB activity or levels. IM saturation is regulated by altering the
404 composition of newly synthesized fatty acids, while OM saturation could be separately
405 regulated by allowing increased transport of more saturated or unsaturated
406 phospholipids as necessary. IM and OM acyl saturation has been studied in several strains
407 of *E. coli* and in *Yersinia pseudotuberculosis* (7, 19-21) and higher saturated fatty acid
408 levels were observed in the OM than in the IM, supporting discrimination of phospholipid
409 transport based on saturation. The IM needs to maintain an appropriate level of fluidity
410 to allow IM proteins to fold and diffuse, to allow diffusion of hydrophobic molecules, to
411 regulate cellular respiration, and to maintain membrane integrity (84, 85). However, the
412 OM is a permeability barrier, a load-bearing element that resists turgor pressure (1-6),
413 and has an outer leaflet consisting of LPS (2, 8). LPS has saturated acyl chains and is largely
414 immobile in *E. coli* (86) and a specific phospholipid saturation level may be necessary to
415 match or counterbalance LPS rigidity. OM phospholipids may also play a role in the
416 physical strength of the membrane. Interestingly, previous work has demonstrated that
417 the tensile strength of the OM is lessened in a *yhdP* mutant (25).

418 Possessing two different phospholipid transporters with different saturation state
419 preferences would allow the cell to adapt OM saturation to changing conditions including
420 temperature shifts, chemical and physical insults, or changes in synthesis of other OM
421 components (e.g., LPS or OMPs). A recent study demonstrated in *Y. pseudotuberculosis*
422 the difference in saturation levels between the membranes is exaggerated at 37 °C
423 compared to 8 °C (21). Thus, conditions where IM and OM saturation are independently
424 regulated exist and this regulation is likely important for optimum fitness of the cells.
425 Transcriptional regulation of *yhdP* and *tamB* has not been thoroughly explored. It seems
426 likely *yhdP* transcription is quite complex with several promoters and transcriptional
427 termination sites (87-89). *tamB* is predicted to be in an operon with *tamA* (which codes
428 for an OMP necessary for TamB function) and *ytfP* (87, 90) and to have a σ^E-dependent
429 promoter (91). The σ^E stress response is activated by unfolded OMP accumulation, and
430 downregulates the production of OMPs and upregulates chaperones and folding
431 machinery (74). It is intriguing to speculate a change in OM phospholipid composition
432 might aid in OMP folding due to altered biophysical properties and/or lipoprotein
433 diffusion. In fact, this could explain the observations that some complicated OMPs fold

434 more slowly in the absence of TamB (34, 44-46). Proper phospholipid composition may
435 be necessary for efficient folding of these OMPs, as it is necessary for the correct folding
436 and topology of some IM proteins (73, 92-95). Recently, it has been demonstrated that
437 the *tamAB* operon is regulated by PhoPQ in *Salmonella enterica* Serovar Typhimurium
438 and that this regulation helps maintain OM integrity in the acidic phagosome
439 environment, perhaps due to indirect effects on OMP folding (96). Thus, changing
440 environments may necessitate changes in phospholipid composition that can be
441 accomplished through differential TamB and, perhaps YhdP, regulation.

442 The mechanism of phospholipid transfer between the IM and OM has been one of the
443 largest remaining questions in gram-negative envelope biogenesis and has remained an
444 area of intense investigation for decades. Furthermore, given the lack of knowledge of
445 this pathway, the role of phospholipid composition in the permeability barrier of the OM,
446 and so the intrinsic antibiotic resistance of gram-negative bacteria, remains unknown.
447 Recent work has begun to elucidate the intermembrane phospholipid transport pathway
448 by identifying YhdP, TamB, and YdbH as proteins capable of transporting phospholipids
449 between the membranes (25, 30, 31). Our work here suggests that YhdP and TamB may
450 have separate roles in phospholipid transport that are differentiated by their preference
451 for phospholipid saturation states and possibly lipid headgroup. Homologs of YhdP and
452 TamB are found throughout *Enterobacterales* and more distantly related members of the
453 AsmA family are widespread in gram-negative bacteria (97). In fact, TamB has recently
454 been shown to play a role in anterograde intermembrane phospholipid transport in the
455 diderm Firmicute *Veillonella parvula* (40, 98) and four AsmA members play a role in
456 phospholipid transport in *Pseudomonas aeruginosa* (41). Structural predictions of YhdP
457 and TamB are strikingly similar between species (32, 33). Given this, it is quite likely similar
458 mechanisms of discrimination in intermembrane phospholipid transfer exist in other
459 species. The data we present here provide a framework for investigation of phospholipid
460 transport and mechanisms differentiating phospholipid transporter function in these
461 species.

462

463

464 **Materials and Methods**

465 **Bacterial strains and Growth Conditions. Table S3** lists the strains used in this study. Most
466 knockout strains were constructed with Keio collection alleles using P1vir transduction
467 (99, 100). New alleles were constructed through λ-red recombineering (101), using the
468 primers indicated in **Table S4**. The FLP recombinase-FRT system was used to remove
469 antibiotic resistance cassettes as has been described (101). *E. coli* cultures were grown in
470 LB Lennox media at 42°C, unless otherwise mentioned. Where noted, LB was
471 supplemented with vancomycin (Gold Biotechnology), bacitracin (Gold Biotechnology),
472 SDS (Thermo Fisher Scientific), EDTA (Thermo Fisher Scientific), oleic acid (Sigma Aldrich),
473 stearic acid (Sigma Aldrich), arabinose (Gold Biotechnology), or glucose (Thermo

474 Scientific). For plasmid maintenance, media was supplemented with 25 µg/mL kanamycin
475 (Gold Biotechnology), 10 or 20 µg/mL chloramphenicol (Gold Biotechnology), or 10 µg/mL
476 tetracycline (Gold Biotechnology) as appropriate.

477 **Plasmid construction.** The pJW15-P_{fabA}, and pJW15-P_{fabA}(-19G>A) reporter plasmids were
478 constructed by amplifying the region upstream of *fabA* from -432 bp to +27 bp relative to
479 the annotated transcriptional start site from wild-type MG1655 or Suppressor 1,
480 respectively, using the Overlap-pJW15-*fabA* FP and RP primers (**Table S4**). pJW15 was
481 amplified using primers Overlap-pJW15-*fabA* FP1 and RP1. The pJW15 plasmid was a kind
482 of gift from Dr. Tracy Raivio (Univeristy of Alberta) (102, 103). The resulting fragments
483 were assembled using HiFi Assembly master mix (New England Biolabs) as per the
484 manufacturer's instructions.

485 **Growth and Sensitivity Assays.** For EOPs assays, cultures were grown overnight, serially
486 diluted, and plated on the indicated media. For *pgsA* depletion, overnight cultures grown
487 in arabinose were washed and diluted 1:100 into fresh LB with 0.2% glucose or arabinose
488 as indicated and grown to OD_{600}=1 before diluting and plating on media with glucose or
489 arabinose respective, as above. EOPs were incubated at 30 °C unless otherwise indicated.
490 Growth curves were performed at the indicated temperature as has been described (43).
491 For CPRG assays (50), strains were streaked on LB plates supplemented with CPRG
492 (40µg/ml) and IPTG (100 µM) incubated overnight at 30°C.

493 **Suppressor isolation and sequencing.** Serially diluted cultures were spread on LB plates
494 and incubated overnight at a 30°C. Colonies that grew at 30°C were isolated and
495 rechecked for cold-resistance through EOP and growth curves. The suppressors were
496 subjected to whole-genome sequencing to identify potential suppressor mutations.
497 Genomic DNA was isolated from the parent and suppressors using a DNeasy Blood and
498 Tissue Kit (Qiagen) as per the manufacturer's instructions. Library preparation and
499 Illumina sequencing were performed by the Microbial Genome Sequencing Center (MiGS,
500 Pittsburgh, PA, USA). Briefly, Illumina libraries were prepared and the libraries were
501 sequenced with paired-end 151 bp reads on a NextSeq 2000 platform to a read depth of
502 at least 200 Mbp. To identify variants from the reference genome (GenBank: U00096.3),
503 reads were trimmed to remove adaptors and the *breseq* software (version 0.35.4) was
504 used to call variants (104). Identified mutations were confirmed with Sanger sequencing.
505 The consensus motif of the FabR binding site of *fabA* was determined using Multiple Em
506 for Motif Elicitation (MEME) tool in the MEME Suite based on the sequence of putative
507 FabR binding sites reported by Feng and Cronan (2011) (64, 105, 106). The ability of the
508 identified P_{fabA} mutation to suppress was confirmed by linking the mutant to *zcb*-
509 3059::Tn*10* (107) and transducing to a clean background.

510 **Lux reporter assays.** Overnight cultures of strains harboring the pJW15-P_{fabA} and pJW15-
511 P_{fabA}(-19G>A) plasmids were sub-cultured at (1:100) into 200 µl of fresh LB broth in a black
512 96-well plate. The plate was incubated in a BioTek Synergy H1 plate reader and the OD_{600}

513 and luminescence intensity were recorded every 2.5 min for 6 hours as described in
514 previously (103, 108). Each biological replicate was performed in technical triplicate.

515 **RNA-seq.** Overnight cultures grown at 42°C were subcultured 1:100 into fresh media and
516 incubated at 42 °C until an OD_{600} of 0.4. Then, the cultures were shifted to a 30 °C water
517 bath for 30 minutes. 500 µL of each culture was immediately fixed in the RNAprotect
518 Bacteria Reagent (Qiagen) as per the manufacturer's instructions. RNA was purified using
519 the RNeasy Kit (Qiagen) with on-column DNase digestion following the manufacturer's
520 protocol for gram-negative bacteria. Library preparation, Illumina sequencing, and
521 analysis of differentially expressed genes were performed by MiGS. Briefly, samples were
522 treated with RNase free DNase (Invitrogen) and library preparation was performed with
523 the Stranded Total RNA Prep Ligation with Ribo-Zero Plus Kit (Illumina). Libraries were
524 sequenced with 2x50 bp reads on a NextSeq2000 (Illumina). Demultiplexing, quality
525 control, and adapter trimming carried out using bcl-convert (Illumina, v3.9.3) and
526 bcl2fastq (Illumina). Read mapping and read quantification were performed with HISAT2
527 (109) and the featureCounts tool in Subreader (110), respectively. Descriptive statistics of
528 the RNA-seq read data can be found in **Table S1**. The raw RNA-seq data is available in the
529 Sequence Read Archive database (SRA) (https://www.ncbi.nlm.nih.gov/sra, BioProject ID
530 PRJNA965821; Reviewer Access).

531 Raw read counts were normalized using the Trimmed Mean of M values algorithm in
532 edgeR (111) and converted to counts per million. The Quasi-Linear F-Test function of
533 edgeR was used for differential expression analysis. Normalized read values and for all
534 genes as well as differential expression analysis statistics can be found in **Dataset S3**.
535 KEGG pathway analysis was conducted using the *"kegga"* function of limma (112).
536 Expression of genes differentially expressed (greater than 2-fold change and $p<0.05$) was
537 subjected to principle component analysis, and pathway and enrichment analysis using
538 the EcoCyc Omics Dashboard (112).

539 **Lipid extraction and TLC.** For thin layer chromatography (TLC) experiments, cultures were
540 grown in LB with 1 mCi/mL ^{32}P until OD_{600} of 0.6-0.8 at the indicated temperature. For
541 temperature downshift experiments, cells were grown at 42 ^{o}C until OD_{600} of 0.2 and then
542 transferred to 30 ^{o}C for 2 hours. For lipid extraction, cells were pelleted and resuspended
543 in 0.2 mL of 0.5 M NaCl in 0.1 N HCl. Lipids were extracted by first adding 0.6 mL of
544 chloroform:methanol (1:2) to create a single-phase solution. After vigorous vortexing for
545 30 minutes, 0.2 mL of 0.5 M NaCl in 0.1 N HCl was added to convert the single-phase
546 solution to a two-phase solution. After centrifugation at 20 000 x g for 5 minutes at room
547 temperature, the lower phase was recovered and used for TLC. Approximately 2,000 cpm
548 of phospholipid extract was subjected to TLC analysis using a HPTLC 60 plate (EMD,
549 Gibbstown, NJ)) developed with either solvent 1: chloroform/methanol/acetic acid
550 [60/25/10 (vol/vol/vol) in **Fig. 2A** or by solvent 2: chloroform/methanol/ammonia/water
551 [65/37.5/3/1] (vol/vol/vol/vol) in **Fig. S4**. Radiolabeled lipids were visualized and
552 quantified using a Phosphoimager Typhoon FLA 9500 (GE). Images were processed and

553 quantified using ImageQuant^{TM} software for scanning and analysis. The phospholipid
554 content is expressed as molecular percentage of the total phospholipids (correcting for
555 the two phosphates per molecule of CL).

556 **Phospholipid composition analysis.** Whole cell lipid extracts were isolated as for TLC
557 temperature downshift experiments without radiolabelling. Absolute amounts of CL, PG,
558 and PE were determined in these lipid extracts using liquid chromatography coupled to
559 electrospray ionization mass spectrometry (LC/MS) in an API 4000 mass spectrometer
560 (Sciex, Framingham, MA, USA) using normal phase solvents as previously published (113).
561 The cardiolipin internal standard $(14:0)_4$CL (Avanti Polar Lipids, Alabaster, AL USA) was
562 added to all samples to quantify CL, PG, and PE with in a single run. Standard curves
563 containing reference standards of all three phospholipids, $(18:1)_4$CL (Avanti Polar Lipids),
564 $16:0_118:1_1$PG and $16:0_118:1_1$PE (Cayman Chemicals, Ann Arbor, MI, USA) were used to
565 quantify the nmol/mg protein for each species (**Dataset 1**) as previously described (114).
566 Percentage values were calculated by dividing the absolute value of that species by the
567 sum of individual molecular species of CL, PG, or PE. The identities of CL species were
568 confirmed using tandem mass spectrometry.
569
570
571 **Acknowledgments**
572
573 We thank members of the Mitchell Lab for productive discussions. We would like to thank
574 Professor Tracy Raivio (University of Alberta) for the kind gift of pJW15 plasmid. This work
575 was funded by the National Institute of Allergy and Infectious Disease under Award
576 Number R01-AI155915 and R01-AI155915-S1 (to A.M.M.), the National Institute of
577 General Medical Sciences under Award Number R01-GM121493 (to M.B.), and Texas
578 A&M University start-up funds (to A.M.M.).
579
580
581 **References**

582 1. Nikaido H. 2003. Molecular basis of bacterial outer membrane permeability
583 revisited. Microbiology and Molecular Biology Reviews 67:593-656.
584 2. Silhavy TJ, Kahne D, Walker S. 2010. The bacterial cell envelope. Cold Spring
585 Harbor Perspectives in Biology 2.
586 3. Henderson JC, Zimmerman SM, Crofts AA, Boll JM, Kuhns LG, Herrera CM, Trent
587 MS. 2016. The power of asymmetry: Architecture and assembly of the Gram-
588 negative outer membrane lipid bilayer. Annual Review of Microbiology 70:255-
589 278.
590 4. Berry J, Rajaure M, Pang T, Young R. 2012. The spanin complex is essential for
591 lambda lysis. J Bacteriol 194:5667-74.

592 5. Rojas ER, Billings G, Odermatt PD, Auer GK, Zhu L, Miguel A, Chang F, Weibel DB,
593 Theriot JA, Huang KC. 2018. The outer membrane is an essential load-bearing
594 element in Gram-negative bacteria. Nature 559:617-621.
595 6. Navarro Llorens JM, Tormo A, Martinez-Garcia E. 2010. Stationary phase in gram-
596 negative bacteria. FEMS Microbiol Rev 34:476-95.
597 7. Lugtenberg EJJ, Peters R. 1976. Distribution of lipids in cytoplasmic and outer
598 membranes of *Escherichia coli* K12. Biochimica et Biophysica Acta (BBA) - Lipids
599 and Lipid Metabolism 441:38-47.
600 8. Kamio Y, Nikaido H. 1976. Outer membrane of *Salmonella typhimurium*:
601 accessibility of phospholipid head groups to phospholipase c and cyanogen
602 bromide activated dextran in the external medium. Biochemistry 15:2561-70.
603 9. Bogdanov M, Pyrshev K, Yesylevskyy S, Ryabichko S, Boiko V, Ivanchenko P,
604 Kiyamova R, Guan Z, Ramseyer C, Dowhan W. 2020. Phospholipid distribution in
605 the cytoplasmic membrane of Gram-negative bacteria is highly asymmetric,
606 dynamic, and cell shape-dependent. Science Advances 6:eaaz6333.
607 10. Benn G, Mikheyeva IV, Inns PG, Forster JC, Ojkic N, Bortolini C, Ryadnov MG,
608 Kleanthous C, Silhavy TJ, Hoogenboom BW. 2021. Phase separation in the outer
609 membrane of *Escherichia coli*. Proceedings of the National Academy of Sciences
610 118:e2112237118.
611 11. Konovalova A, Silhavy TJ. 2015. Outer membrane lipoprotein biogenesis: Lol is
612 not the end. Philosophical Transactions of the Royal Society B: Biological
613 Sciences 370:20150030.
614 12. Konovalova A, Kahne DE, Silhavy TJ. 2017. Outer Membrane Biogenesis. Annu
615 Rev Microbiol 71:539-556.
616 13. Lundstedt E, Kahne D, Ruiz N. 2021. Assembly and maintenance of lipids at the
617 bacterial outer membrane. Chemical Reviews 121:5098-5123.
618 14. John E. Cronan J, Rock CO. 2008. Biosynthesis of membrane lipids. EcoSal Plus 3.
619 15. Jones NC, Osborn MJ. 1977. Translocation of phospholipids between the outer
620 and inner membranes of *Salmonella typhimurium*. Journal of Biological
621 Chemistry 252:7405-7412.
622 16. Donohue-Rolfe AM, Schaechter M. 1980. Translocation of phospholipids from
623 the inner to the outer membrane of *Escherichia coli*. Proceedings of the National
624 Academy of Sciences 77:1867-1871.
625 17. Raetz CR, Kantor GD, Nishijima M, Newman KF. 1979. Cardiolipin accumulation in
626 the inner and outer membranes of *Escherichia coli* mutants defective in
627 phosphatidylserine synthetase. J Bacteriol 139:544-51.
628 18. Langley KE, Hawrot E, Kennedy EP. 1982. Membrane assembly: movement of
629 phosphatidylserine between the cytoplasmic and outer membranes of
630 *Escherichia coli*. J Bacteriol 152:1033-41.
631 19. White DA, Lennarz WJ, Schnaitman CA. 1972. Distribution of lipids in the wall
632 and cytoplasmic membrane subfractions of the cell envelope of *Escherichia coli*.
633 Journal of Bacteriology 109:686-690.

634 20. Ishinaga M, Kanamoto R, Kito M. 1979. Distribution of phospholipid molecular
635 species in outer and cytoplasmic membranes of *Escherichia coli*. The Journal of
636 Biochemistry 86:161-165.
637 21. Davydova L, Bakholdina S, Barkina M, Velansky P, Bogdanov M, Sanina N. 2016.
638 Effects of elevated growth temperature and heat shock on the lipid composition
639 of the inner and outer membranes of *Yersinia pseudotuberculosis*. Biochimie
640 123:103-109.
641 22. Osborn MJ, Gander JE, Parisi E, Carson J. 1972. Mechanism of Assembly of the
642 Outer Membrane of *Salmonella* typhimurium : Isolation and characterization of
643 cytoplasmic and outer membrane. Journal of Biological Chemistry 247:3962-
644 3972.
645 23. Raetz CR, Newman KF. 1979. Diglyceride kinase mutants of *Escherichia coli*: inner
646 membrane association of 1,2-diglyceride and its relation to synthesis of
647 membrane-derived oligosaccharides. J Bacteriol 137:860-8.
648 24. Bogdanov M. 2023. Renovating a double fence with or without notifying the next
649 door and across the street neighbors: why the biogenic cytoplasmic membrane
650 of Gram-negative bacteria display asymmetry? . Emerging Topics in Life Sciences
651 7:137-150.
652 25. Grimm J, Shi H, Wang W, Mitchell AM, Wingreen NS, Huang KC, Silhavy TJ. 2020.
653 The inner membrane protein YhdP modulates the rate of anterograde
654 phospholipid flow in *Escherichia coli*. Proc Natl Acad Sci U S A 117:26907-26914.
655 26. Malinverni JC, Silhavy TJ. 2009. An ABC transport system that maintains lipid
656 asymmetry in the Gram-negative outer membrane. Proceedings of the National
657 Academy of Sciences 106:8009-8014.
658 27. Sutterlin HA, Shi H, May KL, Miguel A, Khare S, Huang KC, Silhavy TJ. 2016.
659 Disruption of lipid homeostasis in the Gram-negative cell envelope activates a
660 novel cell death pathway. Proceedings of the National Academy of Sciences
661 113:E1565-E1574.
662 28. May KL, Silhavy TJ. 2018. The *Escherichia coli* phospholipase PldA regulates outer
663 membrane homeostasis via lipid signaling. mBio 9:e00379-18.
664 29. Tang X, Chang S, Qiao W, Luo Q, Chen Y, Jia Z, Coleman J, Zhang K, Wang T,
665 Zhang Z, Zhang C, Zhu X, Wei X, Dong C, Zhang X, Dong H. 2021. Structural
666 insights into outer membrane asymmetry maintenance in Gram-negative
667 bacteria by MlaFEDB. Nat Struct Mol Biol 28:81-91.
668 30. Ruiz N, Davis RM, Kumar S. 2021. YhdP, TamB, and YdbH are redundant but
669 essential for growth and lipid homeostasis of the gram-negative outer
670 membrane. mBio 12:e02714-21.
671 31. Douglass MV, McLean AB, Trent MS. 2022. Absence of YhdP, TamB, and YdbH
672 leads to defects in glycerophospholipid transport and cell morphology in Gram-
673 negative bacteria. PLOS Genetics 18:e1010096.
674 32. Jumper J, Evans R, Pritzel A, Green T, Figurnov M, Ronneberger O,
675 Tunyasuvunakool K, Bates R, Žídek A, Potapenko A, Bridgland A, Meyer C, Kohl

676 SAA, Ballard AJ, Cowie A, Romera-Paredes B, Nikolov S, Jain R, Adler J, Back T,
677 Petersen S, Reiman D, Clancy E, Zielinski M, Steinegger M, Pacholska M,
678 Berghammer T, Bodenstein S, Silver D, Vinyals O, Senior AW, Kavukcuoglu K,
679 Kohli P, Hassabis D. 2021. Highly accurate protein structure prediction with
680 AlphaFold. Nature 596:583-589.
681 33. Varadi M, Anyango S, Deshpande M, Nair S, Natassia C, Yordanova G, Yuan D,
682 Stroe O, Wood G, Laydon A, Žídek A, Green T, Tunyasuvunakool K, Petersen S,
683 Jumper J, Clancy E, Green R, Vora A, Lutfi M, Figurnov M, Cowie A, Hobbs N,
684 Kohli P, Kleywegt G, Birney E, Hassabis D, Velankar S. 2021. AlphaFold Protein
685 Structure Database: massively expanding the structural coverage of protein-
686 sequence space with high-accuracy models. Nucleic Acids Research 50:D439-
687 D444.
688 34. Josts I, Stubenrauch CJ, Vadlamani G, Mosbahi K, Walker D, Lithgow T, Grinter R.
689 2017. The structure of a conserved domain of TamB reveals a hydrophobic β taco
690 fold. Structure 25:1898-1906.e5.
691 35. Kumar N, Leonzino M, Hancock-Cerutti W, Horenkamp FA, Li P, Lees JA, Wheeler
692 H, Reinisch KM, De Camilli P. 2018. VPS13A and VPS13C are lipid transport
693 proteins differentially localized at ER contact sites. Journal of Cell Biology
694 217:3625-3639.
695 36. Valverde DP, Yu S, Boggavarapu V, Kumar N, Lees JA, Walz T, Reinisch KM, Melia
696 TJ. 2019. ATG2 transports lipids to promote autophagosome biogenesis. J Cell
697 Biol 218:1787-1798.
698 37. Otomo T, Maeda S. 2019. ATG2A transfers lipids between membranes *in vitro*.
699 Autophagy 15:2031-2032.
700 38. Osawa T, Kotani T, Kawaoka T, Hirata E, Suzuki K, Nakatogawa H, Ohsumi Y, Noda
701 NN. 2019. Atg2 mediates direct lipid transfer between membranes for
702 autophagosome formation. Nat Struct Mol Biol 26:281-288.
703 39. Cooper BF, Clark R, Kudhail A, Bhabha G, Ekiert DC, Khalid S, Isom GL. 2023.
704 Phospholipid transport to the bacterial outer membrane through an envelope-
705 spanning bridge. bioRxiv doi:10.1101/2023.10.05.561070:2023.10.05.561070.
706 40. Grasekamp KP, Beaud Benyahia B, Taib N, Audrain B, Bardiaux B, Rossez Y, Izadi-
707 Pruneyre N, Lejeune M, Trivelli X, Chouit Z, Guerardel Y, Ghigo J-M, Gribaldo S,
708 Beloin C. 2023. The Mla system of diderm Firmicute *Veillonella parvula* reveals
709 an ancestral transenvelope bridge for phospholipid trafficking. Nature
710 Communications 14:7642.
711 41. Sposato D, Mercolino J, Torrini L, Sperandeo P, Lucidi M, Alegiani R, Varone I,
712 Molesini G, Leoni L, Rampioni G, Visca P, Imperi F. 2024. Redundant essentiality
713 of AsmA-like proteins in *Pseudomonas aeruginosa*. mSphere 9:e00677-23.
714 42. Mitchell AM, Wang W, Silhavy TJ. 2017. Novel Rpos-dependent mechanisms
715 strengthen the envelope permeability barrier during stationary phase. J Bacteriol
716 199:e00708-16.

717 43. Mitchell AM, Srikumar T, Silhavy TJ. 2018. Cyclic enterobacterial common
718 antigen maintains the outer membrane permeability barrier of *Escherichia coli* in
719 a manner controlled by Yhdp. mBio 9:e01321-18.
720 44. Selkrig J, Mosbahi K, Webb CT, Belousoff MJ, Perry AJ, Wells TJ, Morris F, Leyton
721 DL, Totsika M, Phan M-D, Celik N, Kelly M, Oates C, Hartland EL, Robins-Browne
722 RM, Ramarathinam SH, Purcell AW, Schembri MA, Strugnell RA, Henderson IR,
723 Walker D, Lithgow T. 2012. Discovery of an archetypal protein transport system
724 in bacterial outer membranes. Nature Structural & Molecular Biology 19:506-
725 510.
726 45. Stubenrauch CJ, Dougan G, Lithgow T, Heinz E. 2017. Constraints on lateral gene
727 transfer in promoting fimbrial usher protein diversity and function. Open Biology
728 7:170144.
729 46. Stubenrauch C, Belousoff MJ, Hay ID, Shen H-H, Lillington J, Tuck KL, Peters KM,
730 Phan M-D, Lo AW, Schembri MA, Strugnell RA, Waksman G, Lithgow T. 2016.
731 Effective assembly of fimbriae in *Escherichia coli* depends on the translocation
732 assembly module nanomachine. Nature Microbiology 1:16064.
733 47. Cronan JE. 2021. The *Escherichia coli* FadR transcription factor: Too much of a
734 good thing? Molecular Microbiology 115:1080-1085.
735 48. Nunn WD, Giffin K, Clark D, Cronan JE. 1983. Role for *fadR* in unsaturated fatty
736 acid biosynthesis in *Escherichia coli*. Journal of Bacteriology 154:554-560.
737 49. Rai AK, Mitchell AM. 2020. Enterobacterial common antigen: Synthesis and
738 function of an enigmatic molecule. mBio 11:e01914-20.
739 50. Paradis-Bleau C, Kritikos G, Orlova K, Typas A, Bernhardt TG. 2014. A genome-
740 wide screen for bacterial envelope biogenesis mutants identifies a novel factor
741 involved in cell wall precursor metabolism. PLoS Genet 10:e1004056.
742 51. Ruiz N, Falcone B, Kahne D, Silhavy TJ. 2005. Chemical conditionality: a genetic
743 strategy to probe organelle assembly. Cell 121:307-17.
744 52. Nikaido H, Vaara M. 1985. Molecular basis of bacterial outer membrane
745 permeability. Microbiol Rev 49:1-32.
746 53. Bishop RE. 2008. Structural biology of membrane-intrinsic β-barrel enzymes:
747 Sentinels of the bacterial outer membrane. Biochimica et Biophysica Acta (BBA) -
748 Biomembranes 1778:1881-1896.
749 54. Rowlett VW, Mallampalli V, Karlstaedt A, Dowhan W, Taegtmeyer H, Margolin W,
750 Vitrac H. 2017. Impact of membrane phospholipid slterations in *Escherichia coli*
751 on cellular function and bacterial stress adaptation. J Bacteriol 199.
752 55. Tan BK, Bogdanov M, Zhao J, Dowhan W, Raetz CRH, Guan Z. 2012. Discovery of
753 a cardiolipin synthase utilizing phosphatidylethanolamine and
754 phosphatidylglycerol as substrates. Proceedings of the National Academy of
755 Sciences 109:16504-16509.
756 56. Pluschke G, Hirota Y, Overath P. 1978. Function of phospholipids in *Escherichia*
757 *coli*. Characterization of a mutant deficient in cardiolipin synthesis. Journal of
758 Biological Chemistry 253:5048-5055.

759 57. Nishijima S, Asami Y, Uetake N, Yamagoe S, Ohta A, Shibuya I. 1988. Disruption of
760 the *Escherichia coli cls* gene responsible for cardiolipin synthesis. Journal of
761 Bacteriology 170:775-780.
762 58. Guo D, Tropp BE. 2000. A second *Escherichia coli* protein with CL synthase
763 activity. Biochimica et Biophysica Acta (BBA) - Molecular and Cell Biology of
764 Lipids 1483:263-274.
765 59. Kikuchi S, Shibuya I, Matsumoto K. 2000. Viability of an *Escherichia coli pgsA* null
766 mutant lacking detectable phosphatidylglycerol and cardiolipin. Journal of
767 Bacteriology 182:371-376.
768 60. Suzuki M, Hara H, Matsumoto K. 2002. Envelope disorder of *Escherichia coli* cells
769 lacking phosphatidylglycerol. Journal of Bacteriology 184:5418-5425.
770 61. Shiba Y, Yokoyama Y, Aono Y, Kiuchi T, Kusaka J, Matsumoto K, Hara H. 2004.
771 Activation of the Rcs signal transduction system is responsible for the
772 thermosensitive growth defect of an *Escherichia coli* mutant lacking
773 phosphatidylglycerol and cardiolipin. J Bacteriol 186:6526-35.
774 62. Grabowicz M, Silhavy TJ. 2017. Redefining the essential trafficking pathway for
775 outer membrane lipoproteins. Proceedings of the National Academy of Sciences
776 114:4769-4774.
777 63. Cronan JE, Jr., Gelmann EP. 1973. An estimate of the minimum amount of
778 unsaturated fatty acid required for growth of *Escherichia coli*. J Biol Chem
779 248:1188-95.
780 64. Feng Y, Cronan JE. 2011. Complex binding of the FabR repressor of bacterial
781 unsaturated fatty acid biosynthesis to its cognate promoters. Molecular
782 Microbiology 80:195-218.
783 65. Feng Y, Cronan JE. 2009. *Escherichia coli* unsaturated fatty acid synthesis:
784 Complex transcription of the *fabA* gene and *in vivo* identification of the essential
785 reaction catalyzed by FabB. Journal of Biological Chemistry 284:29526-29535.
786 66. Henry MF, Cronan JE. 1991. *Escherichia coli* transcription factor that both
787 activates fatty acid synthesis and represses fatty acid degradation. Journal of
788 Molecular Biology 222:843-849.
789 67. Henry MF, Cronan JE. 1992. A new mechanism of transcriptional regulation:
790 Release of an activator triggered by small molecule binding. Cell 70:671-679.
791 68. Rock CO, Jackowski S. 1985. Pathways for the incorporation of exogenous fatty
792 acids into phosphatidylethanolamine in *Escherichia coli*. J Biol Chem 260:12720-
793 4.
794 69. Heath RJ, Rock CO. 1996. Roles of the FabA and FabZ β-hydroxyacyl-acyl carrier
795 protein dehydratases in *Escherichia coli* fatty acid biosynthesis. Journal of
796 Biological Chemistry 271:27795-27801.
797 70. Ostrander DB, Sparagna GC, Amoscato AA, McMillin JB, Dowhan W. 2001.
798 Decreased Cardiolipin Synthesis Corresponds with Cytochromec Release in
799 Palmitate-induced Cardiomyocyte Apoptosis. Journal of Biological Chemistry
800 276:38061-38067.

801 71. Lewis RNAH, Zweytick D, Pabst G, Lohner K, McElhaney RN. 2007. Calorimetric,
802 X-Ray Diffraction, and Spectroscopic Studies of the Thermotropic Phase Behavior
803 and Organization of Tetramyristoyl Cardiolipin Membranes. Biophysical Journal
804 92:3166-3177.
805 72. De Siervo AJ. 1969. Alterations in the phospholipid composition of *Escherichia*
806 *coli* B during growth at different temperatures. J Bacteriol 100:1342-9.
807 73. Bogdanov M, Sun J, Kaback HR, Dowhan W. 1996. A Phospholipid Acts as a
808 Chaperone in Assembly of a Membrane Transport Protein. Journal of Biological
809 Chemistry 271:11615-11618.
810 74. Mitchell AM, Silhavy TJ. 2019. Envelope stress responses: balancing damage
811 repair and toxicity. Nature Reviews Microbiology 17:417-428.
812 75. Luevano-Martinez LA, Kowaltowski AJ. 2015. Phosphatidylglycerol-derived
813 phospholipids have a universal, domain-crossing role in stress responses. Arch
814 Biochem Biophys 585:90-97.
815 76. Fernandez M, Paulucci NS, Peppino Margutti M, Biasutti AM, Racagni GE,
816 Villasuso AL, Agostini E, Gonzalez PS. 2019. Membrane Rigidity and Phosphatidic
817 Acid (PtdOH) Signal: Two Important Events in Acinetobacter guillouiae SFC 500-
818 1A Exposed to Chromium(VI) and Phenol. Lipids 54:557-570.
819 77. Shibata A, Ikawa K, Shimooka T, Terada H. 1994. Significant stabilization of the
820 phosphatidylcholine bilayer structure by incorporation of small amounts of
821 cardiolipin. Biochimica et Biophysica Acta (BBA) - Biomembranes 1192:71-78.
822 78. Boscia AL, Treece BW, Mohammadyani D, Klein-Seetharaman J, Braun AR,
823 Wassenaar TA, Klösgen B, Tristram-Nagle S. 2014. X-ray structure,
824 thermodynamics, elastic properties and MD simulations of
825 cardiolipin/dimyristoylphosphatidylcholine mixed membranes. Chemistry and
826 Physics of Lipids 178:1-10.
827 79. Pennington ER, Fix A, Sullivan EM, Brown DA, Kennedy A, Shaikh SR. 2017.
828 Distinct membrane properties are differentially influenced by cardiolipin content
829 and acyl chain composition in biomimetic membranes. Biochimica et Biophysica
830 Acta (BBA) - Biomembranes 1859:257-267.
831 80. Lopes SC, Ivanova G, de Castro B, Gameiro P. 2018. Revealing cardiolipins
832 influence in the construction of a significant mitochondrial membrane model.
833 Biochimica et Biophysica Acta (BBA) - Biomembranes 1860:2465-2477.
834 81. Marr AG, Ingraham JL. 1962. Effect of temperature on the composition of fatty
835 acids in *Escherichia coli*. Journal of Bacteriology 84:1260-1267.
836 82. Garwin JL, Klages AL, Cronan JE. 1980. Beta-ketoacyl-acyl carrier protein
837 synthase II of *Escherichia coli*. Evidence for function in the thermal regulation of
838 fatty acid synthesis. Journal of Biological Chemistry 255:3263-3265.
839 83. de Mendoza D, Klages Ulrich A, Cronan JE. 1983. Thermal regulation of
840 membrane fluidity in *Escherichia coli*. Effects of overproduction of beta-ketoacyl-
841 acyl carrier protein synthase I. Journal of Biological Chemistry 258:2098-2101.

842 84. Knapp BD, Huang KC. 2022. The effects of temperature on cellular physiology.
843 Annual Review of Biophysics 51:499-526.
844 85. Bogdanov M, Umeda M, Dowhan W. 1999. Phospholipid-assisted refolding of an
845 integral membrane protein: Minimum structural features for
846 phosphatidylethanolamine to act as a molecular chaperone. Journal of Biological
847 Chemistry 274:12339-12345.
848 86. Raetz CR, Whitfield C. 2002. Lipopolysaccharide endotoxins. Annu Rev Biochem
849 71:635-700.
850 87. Conway T, Creecy JP, Maddox SM, Grissom JE, Conkle TL, Shadid TM, Teramoto J,
851 Miguel PS, Shimada T, Ishihama A, Mori H, Wanner BL. 2014. Unprecedented
852 high-resolution view of bacterial operon architecture revealed by RNA
853 sequencing. mBio 5:e01442-14.
854 88. Thomason MK, Bischler T, Eisenbart SK, Förstner KU, Zhang A, Herbig A, Nieselt
855 K, Sharma CM, Storz G. 2015. Global transcriptional start site mapping using
856 differential RNA sequencing reveals novel antisense rnas in *Escherichia coli*.
857 Journal of Bacteriology 197:18-28.
858 89. Adams PP, Baniulyte G, Esnault C, Chegireddy K, Singh N, Monge M, Dale RK,
859 Storz G, Wade JT. 2021. Regulatory roles of *Escherichia coli* 5' UTR and ORF-
860 internal RNAs detected by 3' end mapping. eLife 10:e62438.
861 90. Karp PD, Ong WK, Paley S, Billington R, Caspi R, Fulcher C, Kothari A,
862 Krummenacker M, Latendresse M, Midford PE, Subhraveti P, Gama-Castro S,
863 Muñiz-Rascado L, Bonavides-Martinez C, Santos-Zavaleta A, Mackie A, Collado-
864 Vides J, Keseler IM, Paulsen I. 2018. The EcoCyc database. EcoSal Plus
865 8:10.1128/ecosalplus.ESP-0006-2018.
866 91. Huerta AM, Collado-Vides J. 2003. Sigma70 promoters in *Escherichia coli*: specific
867 transcription in dense regions of overlapping promoter-like signals. Journal of
868 Molecular Biology 333:261-278.
869 92. Dowhan W, Bogdanov M. 2009. Lipid-dependent membrane protein
870 topogenesis. Annu Rev Biochem 78:515-40.
871 93. Bogdanov M, Xie J, Heacock P, Dowhan W. 2008. To flip or not to flip: lipid-
872 protein charge interactions are a determinant of final membrane protein
873 topology. J Cell Biol 182:925-35.
874 94. Bogdanov M, Dowhan W. 2012. Lipid-dependent generation of dual topology for
875 a membrane protein. J Biol Chem 287:37939-48.
876 95. Bogdanov M, Dowhan W, Vitrac H. 2014. Lipids and topological rules governing
877 membrane protein assembly. Biochim Biophys Acta 1843:1475-88.
878 96. Ramezanifard R, Golubeva YA, Palmer AD, Slauch JM. 2023. TamAB is regulated
879 by PhoPQ and functions in outer membrane homeostasis during *Salmonella*
880 pathogenesis. J Bacteriol 205:e0018323.
881 97. Szklarczyk D, Gable AL, Nastou KC, Lyon D, Kirsch R, Pyysalo S, Doncheva NT,
882 Legeay M, Fang T, Bork P, Jensen LJ, von Mering C. 2021. The STRING database in

883 2021: customizable protein-protein networks, and functional characterization of
884 user-uploaded gene/measurement sets. Nucleic Acids Res 49:D605-d612.
885 98. Grasekamp KP, Beaud B, Taib N, Audrain B, Bardiaux B, Rossez Y, Izadi-Pruneyre
886 N, Lejeune M, Trivelli X, Chouit Z, Guerardel Y, Ghigo J-M, Gribaldo S, Beloin C.
887 2023. Bridges instead of boats? The Mla system of diderm Firmicute *Veillonella*
888 *parvula* reveals an ancestral transenvelope core of phospholipid trafficking.
889 bioRxiv doi:10.1101/2023.06.30.547184:2023.06.30.547184.
890 99. Baba T, Ara T, Hasegawa M, Takai Y, Okumura Y, Baba M, Datsenko KA, Tomita
891 M, Wanner BL, Mori H. 2006. Construction of *Escherichia coli* K-12 in-frame,
892 single-gene knockout mutants: the Keio collection. Mol Syst Biol 2:2006.0008-
893 2006.0008.
894 100. Silhavy TJ, Berman ML, Enquist LW. 1984. Experiments with gene fusions. Cold
895 Spring Harbor Laboratory.
896 101. Datsenko KA, Wanner BL. 2000. One-step inactivation of chromosomal genes in
897 *Escherichia coli* K-12 using PCR products. Proceedings of the National Academy
898 of Sciences 97:6640-6645.
899 102. MacRitchie DM, Ward JD, Nevesinjac AZ, Raivio TL. 2008. Activation of the Cpx
900 envelope stress response down-regulates expression of several locus of
901 enterocyte effacement-encoded genes in enteropathogenic *Escherichia coli*.
902 Infection and Immunity 76:1465-1475.
903 103. Wong JL, Vogt SL, Raivio TL. 2013. Using reporter genes and the *Escherichia coli*
904 ASKA overexpression library in screens for regulators of the Gram negative
905 envelope stress response. Methods Mol Biol 966:337-57.
906 104. Deatherage DE, Barrick JE. 2014. Identification of mutations in laboratory-
907 evolved microbes from next-generation sequencing data using breseq. Methods
908 Mol Biol 1151:165-88.
909 105. Bailey TL, Elkan C. 1994. Fitting a mixture model by expectation maximization to
910 discover motifs in biopolymers. Proc Int Conf Intell Syst Mol Biol 2:28-36.
911 106. Bailey TL, Johnson J, Grant CE, Noble WS. 2015. The MEME Suite. Nucleic Acids
912 Res 43:W39-49.
913 107. Singer M, Baker TA, Schnitzler G, Deischel SM, Goel M, Dove W, Jaacks KJ,
914 Grossman AD, Erickson JW, Gross CA. 1989. A collection of strains containing
915 genetically linked alternating antibiotic resistance elements for genetic mapping
916 of Escherichia coli. Microbiol Rev 53:1-24.
917 108. Rai AK, Carr JF, Bautista DE, Wang W, Mitchell AM. 2021. ElyC and cyclic
918 enterobacterial common antigen regulate synthesis of phosphoglyceride-linked
919 enterobacterial common antigen. mBio 12:e02846-21.
920 109. Kim D, Paggi JM, Park C, Bennett C, Salzberg SL. 2019. Graph-based genome
921 alignment and genotyping with HISAT2 and HISAT-genotype. Nature
922 Biotechnology 37:907-915.

110. Liao Y, Smyth GK, Shi W. 2013. featureCounts: an efficient general purpose program for assigning sequence reads to genomic features. Bioinformatics 30:923-930.
111. Robinson MD, McCarthy DJ, Smyth GK. 2009. edgeR: a Bioconductor package for differential expression analysis of digital gene expression data. Bioinformatics 26:139-140.
112. Ritchie ME, Phipson B, Wu D, Hu Y, Law CW, Shi W, Smyth GK. 2015. limma powers differential expression analyses for RNA-sequencing and microarray studies. Nucleic Acids Research 43:e47-e47.
113. Sparagna GC, Johnson CA, McCune SA, Moore RL, Murphy RC. 2005. Quantitation of cardiolipin molecular species in spontaneously hypertensive heart failure rats using electrospray ionization mass spectrometry. J Lipid Res 46:1196-204.
114. Hryc CF, Mallampalli VKPS, Bovshik EI, Azinas S, Fan G, Serysheva II, Sparagna GC, Baker ML, Mileykovskaya E, Dowhan W. 2023. Structural insights into cardiolipin replacement by phosphatidylglycerol in a cardiolipin-lacking yeast respiratory supercomplex. Nature Communications 14:2783.

Figures and Tables

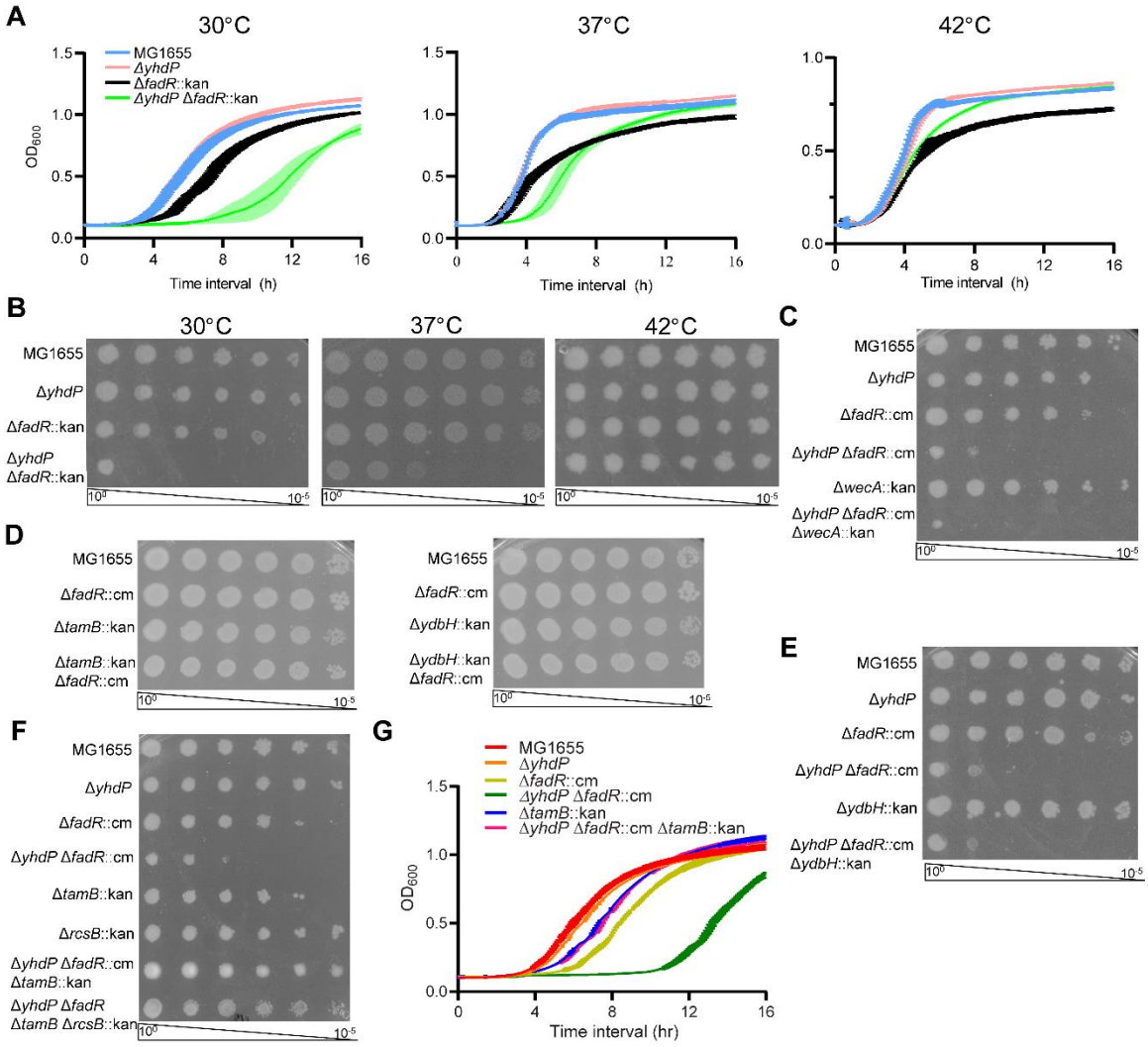

Figure 1. Deletion of *yhdP* and *fadR* causes synthetic cold sensitivity due to impairment of TamB function. (A) The Δ*yhdP* Δ*fadR* strain had impaired growth at lower temperatures. **(B)** EOPs were performed to confirm the growth defect of the Δ*yhdP* Δ*fadR* strain. **(C-F)** EOPs were performed at 30 °C to assess cold sensitivity. **(C)** The growth of the Δ*yhdP* Δ*fadR* strain was not affected by the loss of ECA (Δ*wecA*). **(D)** Neither a Δ*tamB* Δ*fadR* strain nor a Δ*ydbH* Δ*fadR* strain exhibited cold sensitivity. **(E)** Deletion of *ydbH* did not suppress cold sensitivity in the Δ*yhdP* Δ*fadR* strain. **(F)** Deletion of *tamB* completely suppressed cold sensitivity in the Δ*yhdP* Δ*fadR* strain and the Rcs stress response was not necessary for this suppression. **(G)** Growth curves were performed at 30 °C . The Δ*tamB* and the Δ*yhdP* Δ*fadR* Δ*tamB* strain grew equally well, indicating suppression is unlikely to result from slow growth. Quantitative data are shown as the mean of three biological replicates ± the SEM. Images are representative of three independent experiments.

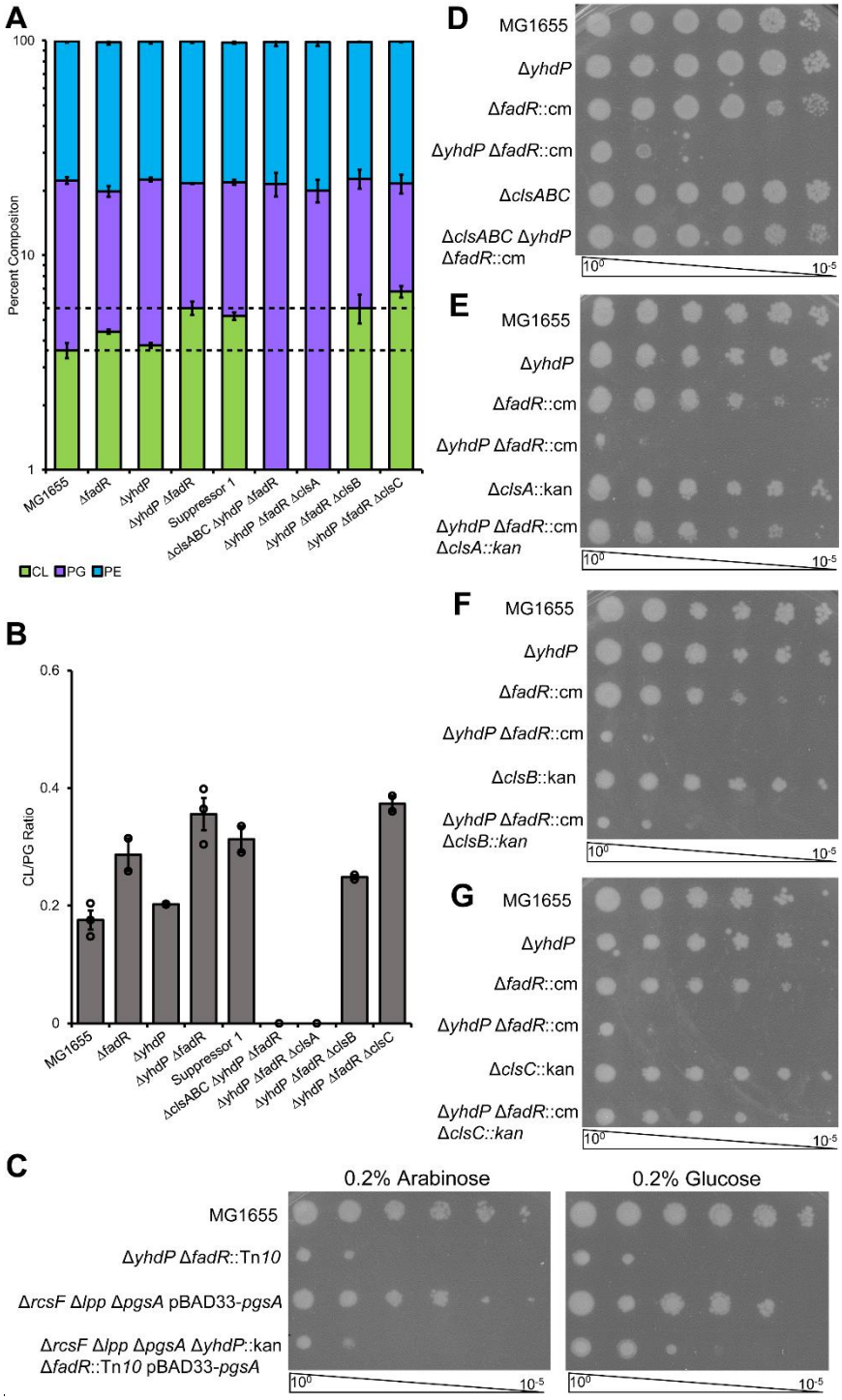

Figure 2. Increased cardiolipin levels are necessary for cold sensitivity of the Δ*yhdP* Δ*fadR* strain. (A-B) Thin layer chromatography (TLC) of lipid extracts was performed for the indicated cultures grown to log phase at 42 °C then transferred to 30 °C for 2 hours before analysis. **(A)** Relative phospholipid levels were calculated. The Δ*yhdP* Δ*fadR* strain shows increased levels of CL and a concomitant decrease in PG levels, increasing the ratio

964 of CL to PG (B). Data are averages of two to three biological replicates ± the SEM. For
965 ratios individual data points are indicated with open circles. **(C-G)** Growth effects of
966 altered phospholipid levels were investigated by EOP. Images are representative of three
967 independent experiments. **(C)** PgsA depletion strains in a background where *pgsA* is non-
968 essential were used to assay the effect of lowering PG and CL levels on cold sensitivity.
969 Arabinose induces expression of *pgsA* while glucose represses. Lowering PG and CL levels
970 partially suppressed cold sensitivity. **(D)** Deletion of the three CL synthases, *clsA*, *clsB*, and
971 *clsC*, suppressed cold sensitivity of the Δ*yhdP* Δ*fadR* strain. **(E)** Deletion of *clsA* also
972 suppressed cold sensitivity. **(F)** Deletion of *clsB* does not suppress cold sensitivity, while
973 deletion of *clsC* (F) does.
974
975

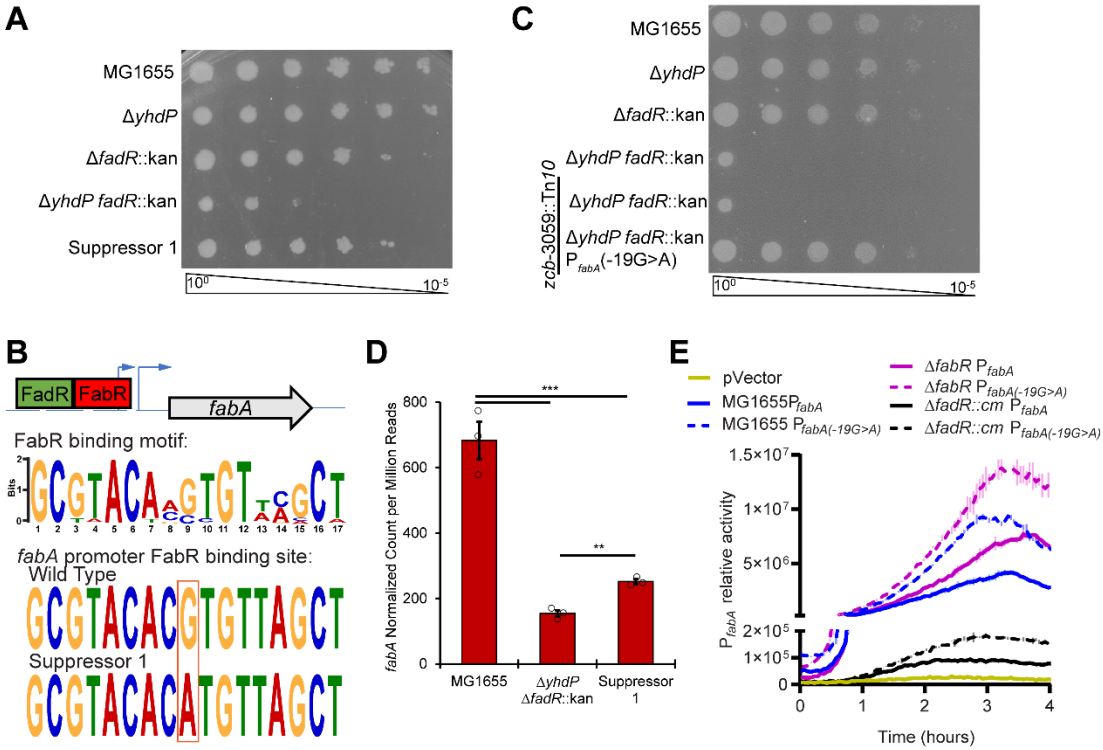

Figure 3. Cold sensitivity can be suppressed by increasing *fabA* expression. (A) The cold sensitivity of a spontaneous suppressor of Δ*yhdP* Δ*fadR* cold sensitivity was tested by EOP. The suppressor returned growth to the level of the Δ*fadR* mutant. **(B)** A diagram of the promoter region of *fabA* is shown with its transcriptional start sites (blue arrows) and regulator binding sites (boxes). FadR acts as an activator while FabR acts as a repressor. The motif of the FabR binding site, generated using MEME, is shown with the sequences of the parent strain and of Suppressor 1. **(C)** The P_{fabA}(-19G>A) mutation was linked to a Tn*10* and transferred to the Δ*yhdP* Δ*fadR* strain by transduction. The Δ*yhdP* Δ*fadR* strain with P_{fabA}(-19G>A) was not cold sensitivity, confirming suppression. **(D)** *fabA* RNA levels are shown. Bars are the mean of three biological replicates ± the SEM. Individual data points are shown as open circles. ** $p<0.005$, *** $p<0.0005$ by quasi-linear F-test. Data are from the RNA-seq experiment in Figure 5 and *fabA* data are also shown in Figure 5F. **(E)** Luciferase reporters of wild-type and mutant *fabA* promoter activity were constructed. The mutation caused similar fold increases in P_{fabA} activity in all strain backgrounds. Data are luminescence relative to OD_{600} and are shown as the average of two biological replicates ± the SEM.

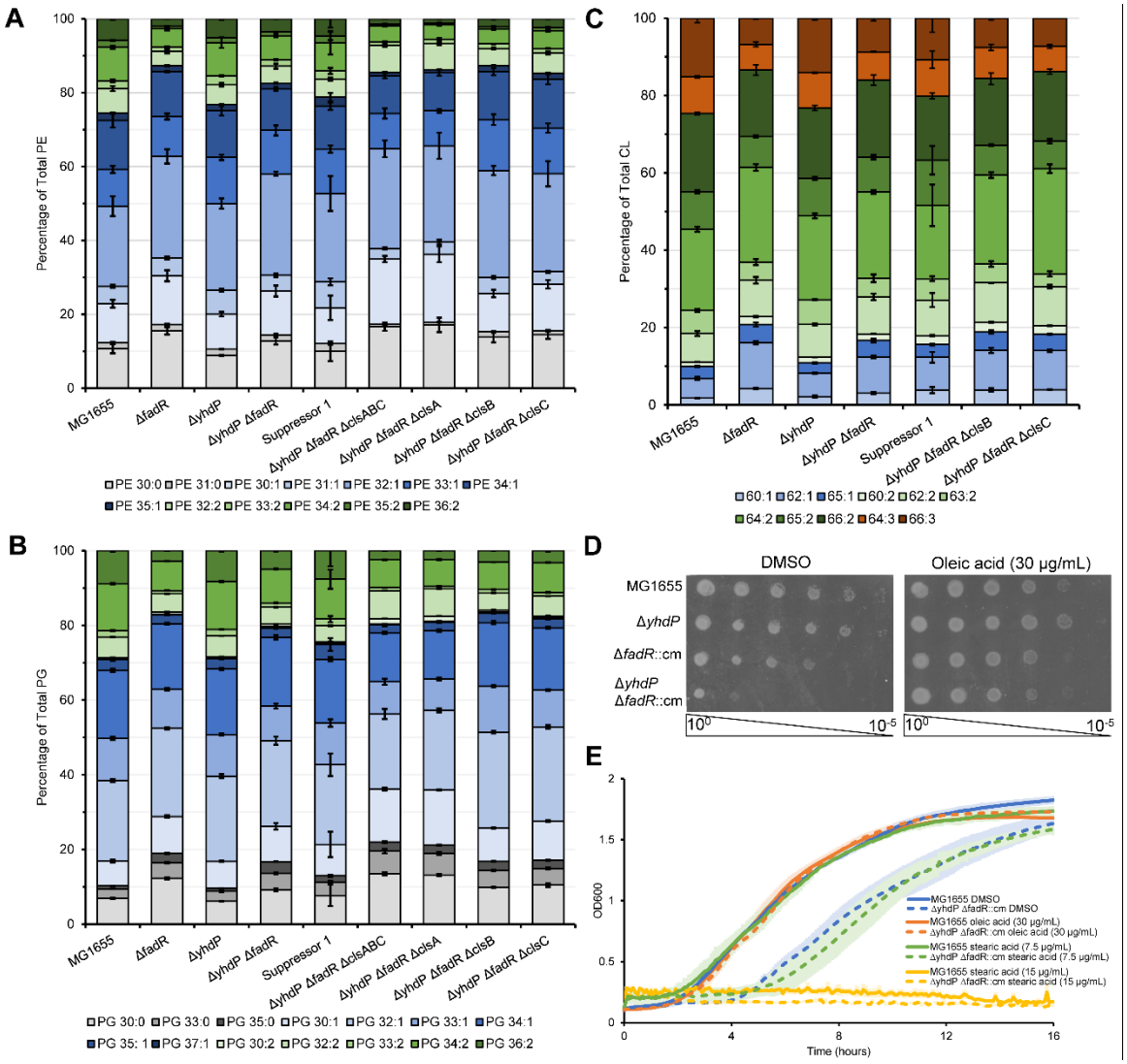

Figure 4. Decreasing fatty acid saturation suppresses Δ*yhdP* Δ*fadR* cold sensitivity. (A-C) Lipid were extracted from cells grown to OD_{600} 0.2 at 42 °C then shifted to 30 °C for 2 hours before harvest. LC/MS was performed on lipid extracts using absolute quantification and the percentage of each specific species of PE (A), PG (B), and CL (C) was calculated using the sum of all molecular species detected. CL is not shown for Δ*clsABC* and Δ*clsA* strains due to low CL levels. Suppressor 1 trends towards decreased saturation compared to its parent strain (Δ*yhdP* Δ*fadR*). Data for phospholipids without unsaturations are shown in grey, with one unsaturation in blue, with two unsaturations in green, with three unsaturations in orange. Data for phospholipids with longer acyl chains are shown in darker colors. Data are the average of three biological replicates ± the SEM. Phospholipids with odd chain lengths and unsaturations may have either odd chain or cyclopropyl fatty acids. **(D)** EOPS were performed on media supplemented with oleic acid or a vehicle control. Oleic acid suppresses the cold sensitivity of the Δ*yhdP* Δ*fadR* strain. **(E)** Growth curves of the indicated strains were performed in the presence of oleic

1010 acid, stearic acid, or a vehicle control. Oleic acid suppressed the cold sensitivity of the
1011 Δ*yhdP* Δ*fadR* strain while stearic acid did not. Data are the average of three biological
1012 replicates ± the SEM.
1013

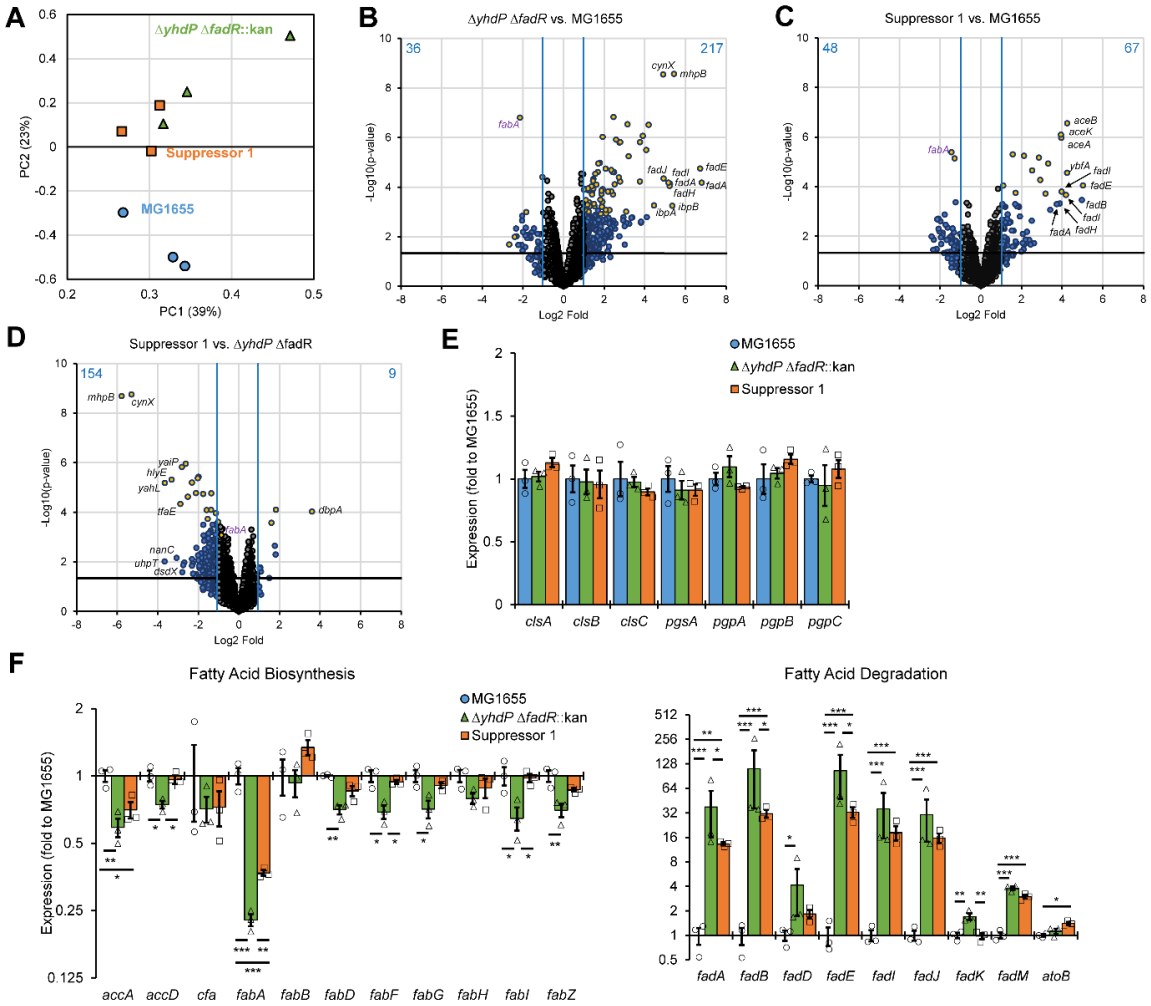

Figure 5. Transcriptional landscape of the Δ*yhdP* Δ*fadR* and suppressed strain. Three biological replicates of the indicated strains were grown at 42 °C to mid-log then transferred to 30 °C for 30 minutes before harvesting RNA and performing RNA-seq. Differential expression was calculated based on a greater than 2-fold change in expression and a p value of less than 0.05 by quasi-linear F-test. **(A)** PCA was performed on the expression of all genes differentially expressed between any groups of samples. Suppressor 1 and the Δ*yhdP* Δ*fadR* strain grouped closer together than to the wild-type strain, although Suppressor 1 was closer to wild type than the Δ*yhdP* Δ*fadR* strain. **(B-D)** Volcano plots show the average fold change and significance of expression changes between the Δ*yhdP* Δ*fadR* strain and wild-type MG1655 (B), Suppressor 1 and wild-type MG1655 (C), and Suppressor 1 and the Δ*yhdP* Δ*fadR* strain (D). Genes with changes greater than 2-fold are shown in blue, while genes with changes less than 2-fold are shown in grey. Genes with a q-value (false discovery rate) of less than 0.05 are shown in yellow. Blue lines indicate a 2-fold change and dotted line indicates p>0.05. The number of up or down regulated genes is indicated in blue. The names of the 10 genes with the largest changes are called out. More genes were up-regulated then down regulated in the Δ*yhdP* Δ*fadR* strain and Suppressor 1 vs. wild type. More genes were down regulated in

1032 Suppressor 1 compared to the Δ*yhdP* Δ*fadR* strain. **(E)** Relative expression of genes in the
1033 CL synthesis pathway is shown as averages ± the SEM and individual data points. No
1034 significant changes were evident. **(F)** Relative expression of genes in the fatty acid
1035 synthesis and degradation pathways is shown as averages ± the SEM and individual data
1036 points. A general normalizing of these pathways occurred in Suppressor 1 compared to
1037 the Δ*yhdP* Δ*fadR* strain; however, the most significant change was in the expression of
1038 *fabA*. * $p<0.05$, ** $p<0.005$, *** $p<0.0005$ by quasi-linear F-test.
1039

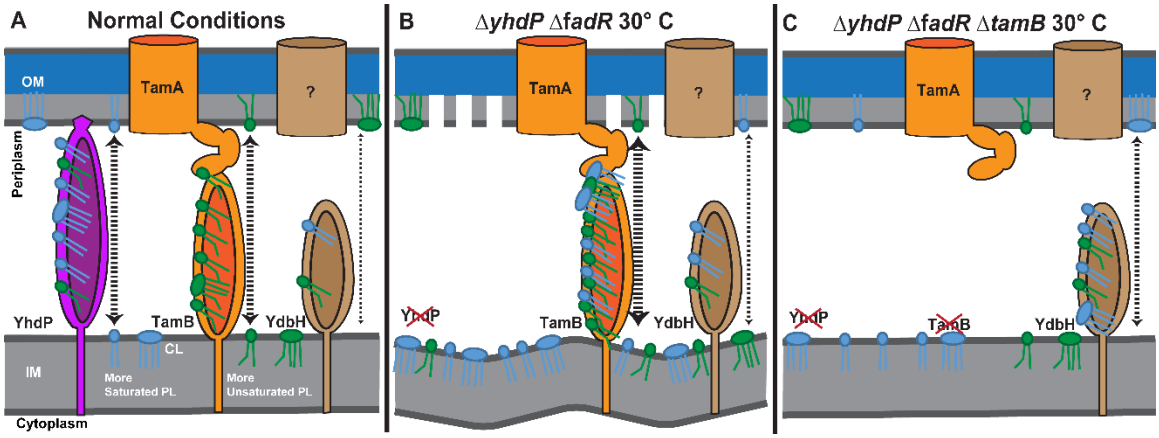

Figure 6. Model for the role of YhdP and TamB in phospholipid transport. Our data can be explained by the following model of phospholipid transport. **(A)** In normal conditions, YhdP is mainly responsible for the transport of phospholipids with more saturated fatty acid chains between the IM and OM. TamB shows a strong preference for transporting phospholipids with more unsaturated fatty acids, with YdbH playing a minor role in phospholipid transport. **(B)** In the Δ*yhdP* Δ*fadR* strain, YhdP is not available to transport more saturated phospholipids and the proportion of both saturated fatty acids and cardiolipin is increased, especially at low temperature. The fluidity of the membrane is also lessened by the low temperature. In these conditions, transport of phospholipids between the membranes is impeded, due to clogging of TamB by a combination of less saturated phospholipids and/or bulky and highly disordered CL. This leads to a lethal lack of phospholipids in the OM and overabundance of phospholipids in the IM. **(C)** When *tamB* is deleted in the Δ*yhdP* Δ*fadR* strain, the clogging of TamB is relieved, and the cell relies on YdbH for phospholipid transport overcoming the cold sensitivity. PL: phospholipid